SC

DEVELOPMENT OF ELECTRIC PROBES TO DETECT PHASE CHANGE AT A HEATED SURFACE

by

Helmy S. Ragheb

Thesis submitted to the School of Graduate Studies of the University of Ottawa as partial fulfillment of the requirements for the degree of Master of Applied Science in Mechanical Engineering.

UNIVERSITAS SCIENTIAE OTTAVIENSIS

ACKNOWLEDGMENTS

I wish to express my appreciation to Dr. S.C. Cheng, who initiated the present investigations, for his support, guidance and encouragement.

I would like to pay particular thanks to Dr. D.C. Groeneveld, of A.E.C.L., who provided countless thoughtful suggestions and ideas throughout this work.

An expression of thanks is extended to Atomic Energy of Canada Limited, and Argonne National Laboratory, Illinois, U.S.A., for their financial support.

Special thanks and gratitude to Mr. W. Ng, who has extended much of his precious time in assistance and providing valuable ideas.

I would also like to convey my appreciation to Mr. K.T. Heng, for his valuable advice in programming.

I am indebted to the technical staff of the Mechanical Engineering workshop for their cooperation, and I wish to extend special thanks to Mr. G. Spak.

ABSTRACT

Two types of electric resistance probe have been developed to detect the rewetting of a heated surface, during quenching experiments. Measurements of electric resistance were made using two different methods:

i. Two-Electrode measurement, through a thermocouple probe
ii. Probe-to Wall measurement, through a zirconium-platinum probe.

Forced vertical flow experiments were conducted for water at atmospheric pressure, mass fluxes at 25,000 and 50,000 lbm/hr-ft^2 and inlet subcooling ranging from 0 to 70^{o}F. These experiments were preceded by a pool boiling experiment to relate visually the probe output signals to different boiling regimes.

The zirconium-platinum probe showed many advantages over the thermocouple probe and could detect the onset of rewetting at 440-480^{o}F. The maximum heat flux point was also detected by both types of probe and was found to be in good agreement with those available from boiling curves. Several boiling phenomena recorded by the probes, are discussed. Finally, recommendations are made for alternative methods of detecting the transition from film boiling to nucleate boiling during a quenching process.

Contents

LIST OF FIGURES

NOMENCLATURE

A	area $[ft^2]$;
c_p	specific heat at constant pressure $[Btu/lb_m\text{-}^oF]$;
h	heat transfer coefficient at outer wall $[Btu/hr\text{-}ft^2\text{-}^oF]$;
k	thermal conductivity $[Btu/hr\text{-}ft\text{-}^oF]$;
L	length of test section $[ft]$;
Q	heat content of test section at time t $[Btu]$
q	heat flux $[Btu/hr\text{-}ft^2]$;
r	radial coordinate $[ft]$;
T	temperature $[^oF]$;
ΔT	Wall superheat $(T_w\text{-}T_s)$ $[^oF]$;
t	time $[hr]$;
α	thermal diffusivity $[ft^2/hr]$;
Δr	regular radial increment $[ft]$;
Δr_o	radial distance between inner wall and location of T.C. (Fig. 26) $[ft]$;
ρ	density $[lb_m/ft^3]$.

Subscripts

amb	ambient;
c	critical point of substance;
CHF	critical heat flux;
calc.	calculated;
cr1	boiling crisis (at max. heat flux)
cr2	boiling crisis (at min. heat flux)

NOMENCLATURE (cont'd.)

exp.	experimental
i	i th nodal point;
in	inner wall;
L	liquid;
o	location of T.C.
out	outer wall;
s	saturation;
SUB	subcooling;
w	wall;
-1	nodal point at inner wall.

CHAPTER 1

INTRODUCTION

1.1 - General:

During emergency core cooling in a water cooled nuclear power reactor, the heat transfer mode changes from film boiling to transition boiling at the minimum heat flux point, and from transition boiling to nucleate boiling at the maximum heat flux point. In both cases, the thermal analysis requires precise knowledge of the conditions of the boiling crisis (CHF or maximum heat flux) and rewetting. Although one can obtain these conditions from a full boiling curve* (Fig. 1), the problem is that the boiling curves of flow conditions of interest are rarely available. Hence, an alternative method of detecting CHF and rewetting points is very important.

---

*Although the minimum heat flux is depicted as a point in Fig. 1 (point A), in reality there is a region or a domain where it occurs [25].

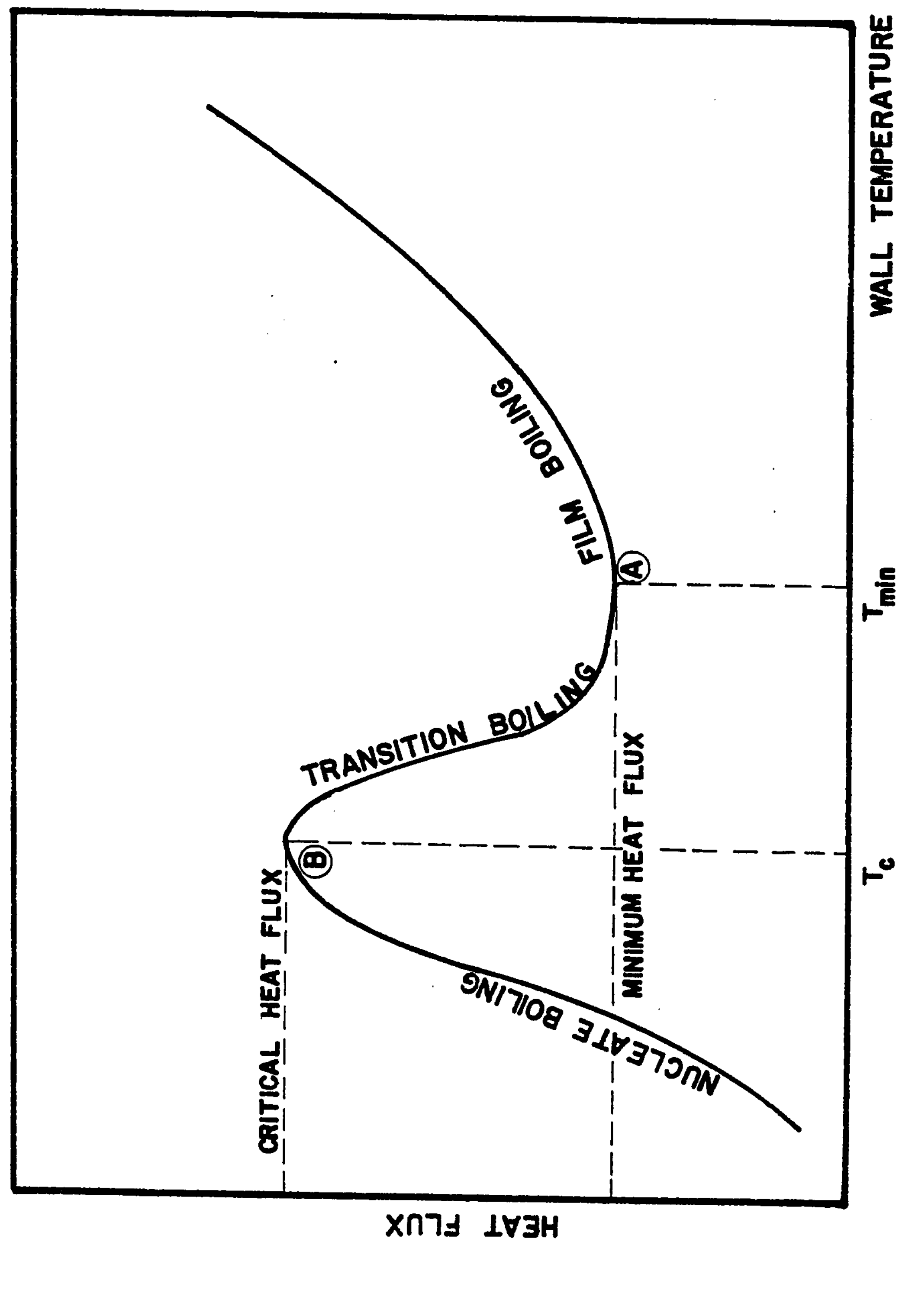

FIG. I BOILING CURVE

Since both boiling crisis and rewetting points are associated with a phase change, in this thesis, a technique has been developed to detect the phase change at the heated surface by means of electric resistance measurements. It can also be used to check both CHF and rewetting points for an existing boiling curve.

Systems used for measurement of transition boiling data can either be steady-state or transient. In the current study, transition boiling data have been measured through a transient system, in which a copper block was employed as a test section. The high thermal capacity of the copper block will permit longer transition time during a quenching process, and permits the block to act in a pseudo steady-state manner.

The high temperatures and severe transients associated with a quenching process, made it very difficult to perform electric resistance measurements at the heated surface, especially through thick-walled tubes. Therefore, two special types of electric probes are designed for this study, a thermocouple probe,* and a zirconium-platinum probe.

---

*Thermocouple junction with the tip removed to expose the leads.

1.2 - Survey of Literature:

1.2.1- The Maximum and Minimum Heat Flux Points:

It was a well known fact that the heat flux, q, transmitted from a metallic surface to boiling water, increases with their temperature difference ΔT. However, it was not known whether heat flux, q, had a maximum and minimum value until 1935, when Nukiyama [1], observed the existence of several modes of boiling over an electrically heated wire submerged in a pool of water. In his experiment it was found that the heat flux, q, reached its maximum value at point (b) as shown in Fig. 2, when the wire was heated in pool boiling. Beyond point (b), the fluid could not accept heat as fast as being supplied by constant electric heating. Thus, the heat added was stored partially in the wire, causing the surface temperature to rise drastically from (b) to (a), and the wire was melted. On the other hand, it was shown by experiment - using a platinum wire to prevent melting - that at very high temperatures, q could be large due to radiation along path (a-d). Therefore, Nukiyama expected that q has

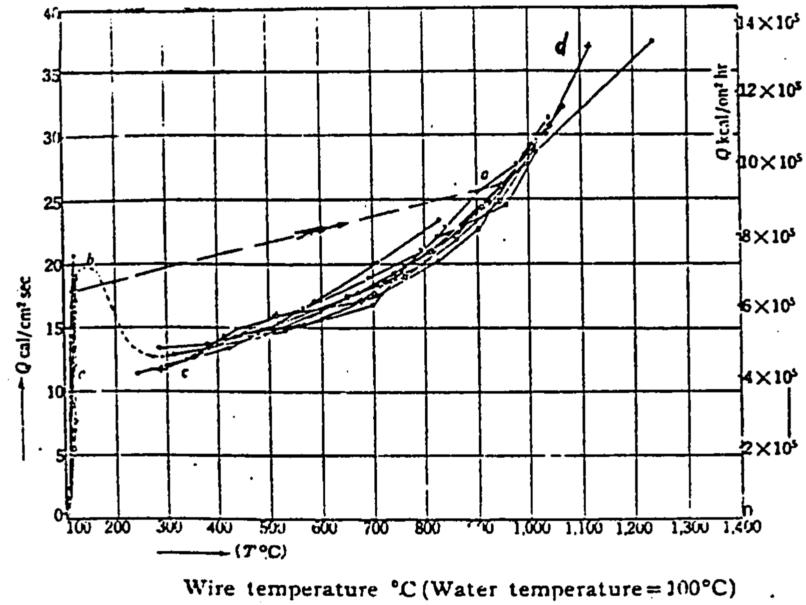

Fig.(2) The Boiling Curve of Nukiyama [1]

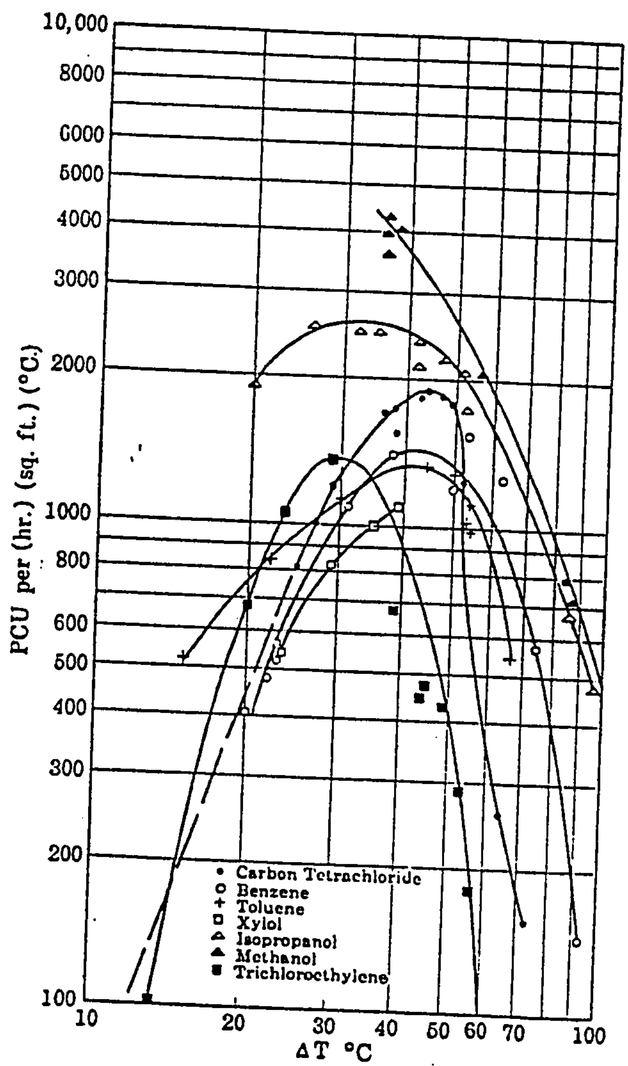

Fig. (3)

Experimental Data in the Transition region reported by Drew and Mueller [2].

a minimum value between (a) and (b).

Indeed, by decreasing the electric power, the change of q traced along a smooth curve (a - c), followed by a sudden jump (c - e). He referred to the dotted line (c - b) as an unstable region (transition region).

1.2.2 - The Transition Boiling Region:

The work of Nukiyama led Drew and Mueller [2], to hypothesize the existence of the transition boiling region. In their study on the behavior of boiling organic liquids, they could identify a transition range, just beyond the maximum heat flux point, in which a mechanism distinct from film and nucleate boiling exists. They reported the first data in transition boiling region as shown in Fig. 3.

1.2.3 - Measurements of Transition Boiling Data Using the Transient Method:

Transition boiling data in forced

convective flow can only be obtained through a temperature controlled system, or during transient tests. A number of transition boiling experiments have been reported in the literature, an excellent review of which was made by Groeneveld [3].

In the transient system, the test section is heated to a high temperature before introducing the flow, thus allowing the film boiling to establish. By cooling down the test section, a temperature history (cooling curve) can be recorded. A boiling curve can therefore be constructed, based on the temperature history, using inverse heat transfer method. If, however, the temperature distribution is assumed to be uniform across the wall (lumped parameter model), a crude boiling curve can be obtained by differentiating the temperature-time recording (see Fig. 4).

The "Transient method" has been used by Iloeje, et al. [4,5] and Collier [6], to obtain transition data in forced vertical flow. The same technique was used in pool boiling by Tachibana [7]. The use of the transient method in the case of a

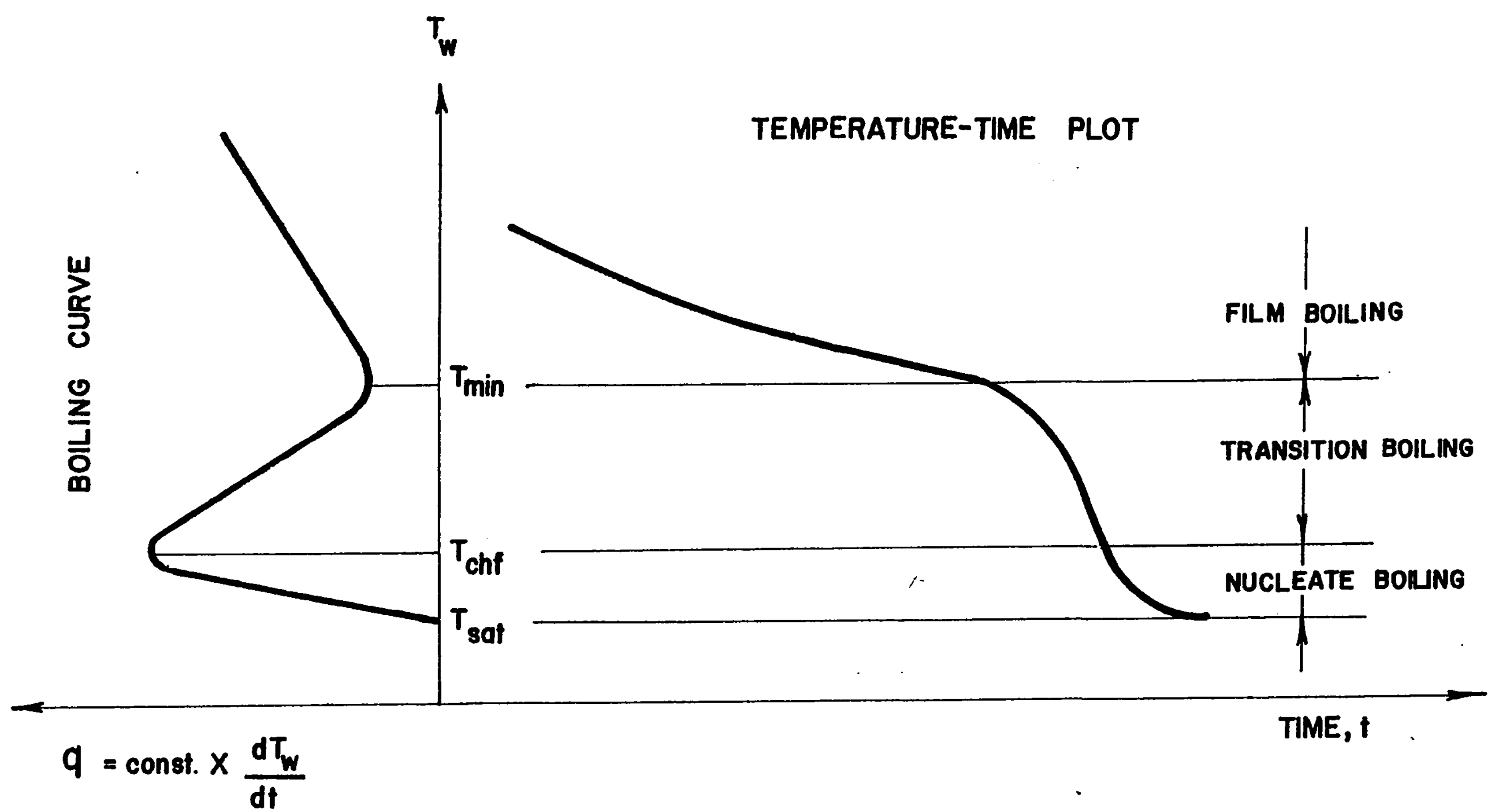

FIG. 4 DERIVATION OF BOILING CURVE FROM TEMPERATURE - TIME PLOT

thick-walled channel, has been reported by Cheng, et al. [8], who constructed the boiling curve using the concept of rate of change of heat content within the test section.

During a quenching process, the transition occurs from film boiling to nucleate boiling, in the manner in which it would occur during Emergency Core Cooling (ECC) in a nuclear reactor. This type of transition* is associated with the collapse of the vapor film next to the heated surface. In order to predict conditions at the start and end of the collapse (q min., T min., q max., and T max.), it is necessary that its mechanisms be understood.

1.2.4 - Mechanisms of Collapse:

To predict the process of collapse, a number of models have been suggested in the available literature, yet no complete answer exists.

---

*Some literature calls this "Leidenfrost" transition (see ref. [25], p. 115)

Iloeje et al. [6] isolated three controlling mechanisms for forced convective rewet*. These are, impulse cooling collapse, axial conduction controlled rewet, and dispersed flow rewet.

1.2.4.1 - Impulse Cooling Collapse:

At a temperature higher than T_{rewet}**, the fluid is separated from the wall by a vapor film. If the wall temperature is lowered, the film thickness decreases, so that the crests of the wavy fluid-vapor interface may contact the wall. These repeated contacts, during a quenching process, decrease the wall temperature and allow rewetting.

This model has been proposed by Kalinin [9], who performed a conduction analysis to obtain the temperature of beginning and ending of the film boiling

---

*Surface rewetting refers to the phenomenon of establishing liquid contact with a solid surface whose initial temperature is greater than the rewetting temperature.

**T_{rewet} is the temperature up to which the surface may wet.

crisis (Collapse of vapor film) T_{cr2} and T_{cr1}. In order for his analysis to be useful, the frequency of contacts before collapse needs to be known. The difficulty in obtaining such information would appear to make his solution useless. However, his solution showed that T_{cr2} and T_{cr1} increase with increasing the group parameter $\sqrt{(\rho C_p K)_w}$. Therefore, he conducted experiments to study the effect of thermophysical properties of wall material on T_{cr2} and T_{cr1}, using annular channels made of different materials, and cooled by different liquids, in both pool and forced convective boiling. His data in Fig. 5 was correlated in terms of the ratio $\sqrt{\frac{(\rho C_p K)_L}{(\rho C_p K)_w}}$. The wall temperatures corresponding to the minimum and maximum heat flux in forced convective flow, can be obtained from his empirical relations:

$$\frac{\Delta T_{cr1}}{T_c - T_L} = 0.1 + 1.5 \left[\frac{(\rho C_p K)_L}{(\rho C_p K)_w}\right]^{0.25} + 0.6 \frac{(\rho C_p K)_L}{(\rho C_p K)_w} \qquad (1.1)$$

$$\frac{\Delta T_{cr2}}{\Delta T_{cr1}} = 1.65 \qquad (1.2)$$

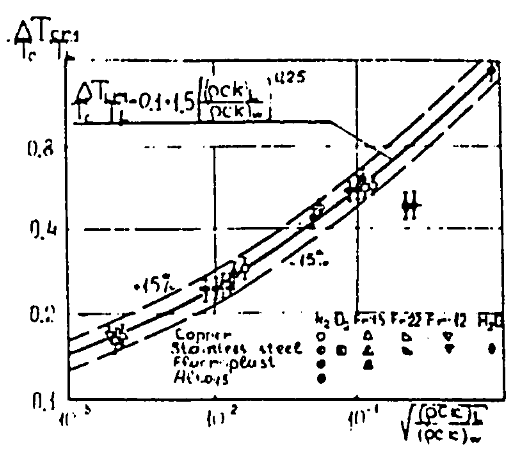

a Generalization of experimental data on temperature of ending film boiling crisis under channels flow

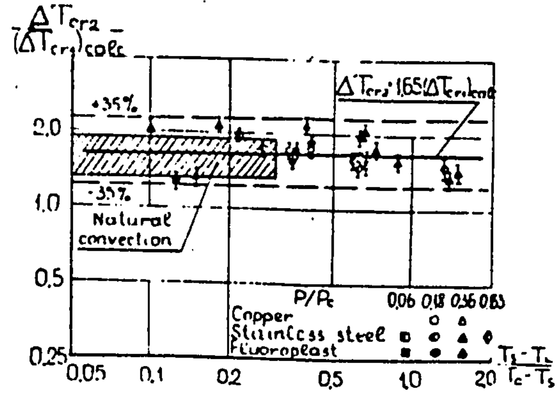

b Generalization of data on T_{cr2} in channels

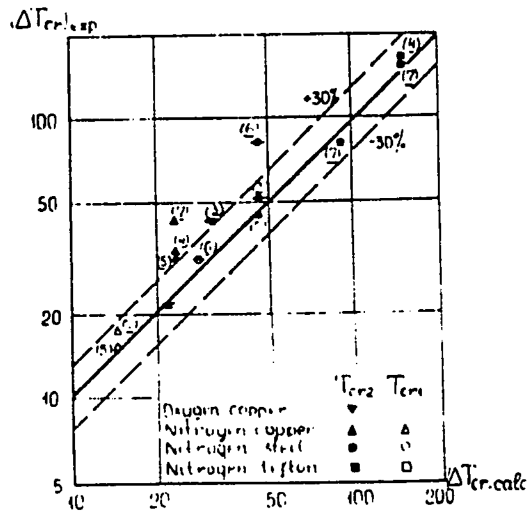

C Comparision of experimental data of various authors with results calculated according to formulae (1.1), (1.2)

FIG. 5 EXPERIMENTAL DATA OF "KALININ, et al."

The dependence of the critical temperatures on the group parameter $\sqrt{PC_pK}$ is due to the assumption that the heat transfer over the contact region is controlled by pure conduction. A local decrease of the temperature over this region depends on the rate of heat supplied from the heater material to the contact region. Therefore, if the material is highly conductive, the heat supply will be at such a high rate as to delay rewetting to a lower temperature.

In general, there are two reasons why this model seems to be poor. Kalinin did not reveal any effect of flow velocity on the maximum and minimum heat flux temperatures. The second reason is that there may be some error in ignoring the axial conduction.

1.2.4.2 - <u>Axial Conduction Controlled Rewet</u>

Based on their visual observation of the hydrodynamic conditions existing at the minimum heat flux, Simon and Simoneau [10], suggested that the transition from film boiling to nucleate boiling is controlled by axial conduction. Wall conduction transfers heat from the film boiling side to the nucleate boiling side (Fig. 6) and causes the surface temperature to drop. Transition will occur at a position on the wall where the rewetting temperature is reached.

In their analysis, they assumed that the rewetting temperature was equivalent T_{min}, and used the theoretical equation of Spieglar et al. [11]:

$$\frac{T_{wet}}{T_c} = 0.13 \frac{P}{P_c} + 0.84 \qquad (1.3)$$

The above equation implies that both minimum heat flux and rewetting temperature are solely determined by the thermodynamic properties of the boiling fluid. Experimental results showed that T_{min} varies considerably for the same fluid and system pressure, and in some cases much higher than T_c. For these reasons, one would conclude that T_{min} is not a thermodynamic property of the fluid.

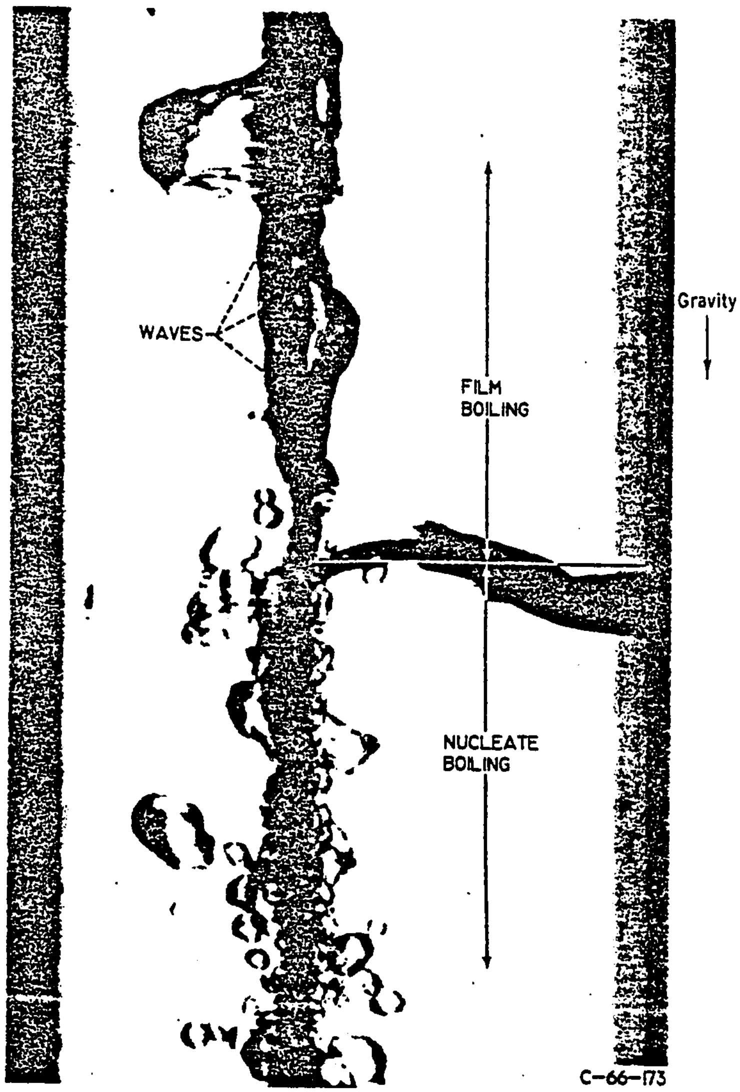

- Nucleate transition region in vicinity of transition heat flux (upward flow). Velocity, 0.27 m/sec; heat flux, 6.9×10^4 w/m^2.

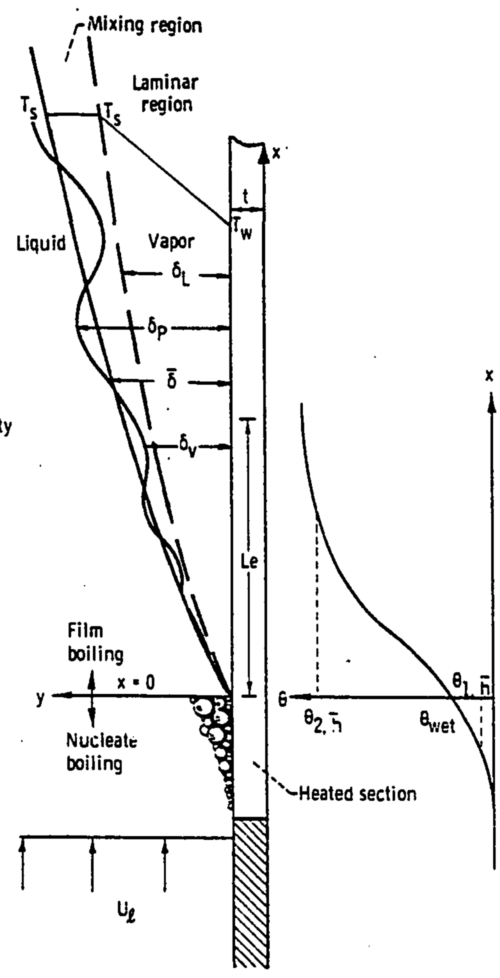

Film boiling model.

FIG. 6 AXIAL CONDUCTION CONTROLLED REWET

FROM SIMON, et al. [10]

1.2.4.3 - Dispersed Flow Rewet

The variation of T_{min} for the same fluid and system pressure has been discussed by Iloeje et al. [6], who attributed this variation to surface effects, namely scale deposits, and surface roughness. They took the view that the rewet temperature predicted by Spiegler et al. [11] might be a thermodynamic property, but not T_{min}.

In an attempt to encounter all the observed effects on ΔT_{min}, they proposed a dual mode heat transfer model. Heat transfer to the flow is a sum of two components:

1. Heat transfer to droplets of water hitting the wall.

2. Heat transfer to vapor assuming no effect of the existence of droplets.

The sum of these two components give the total q and indicates ΔT_{min}. Fig. 7 shows the change of

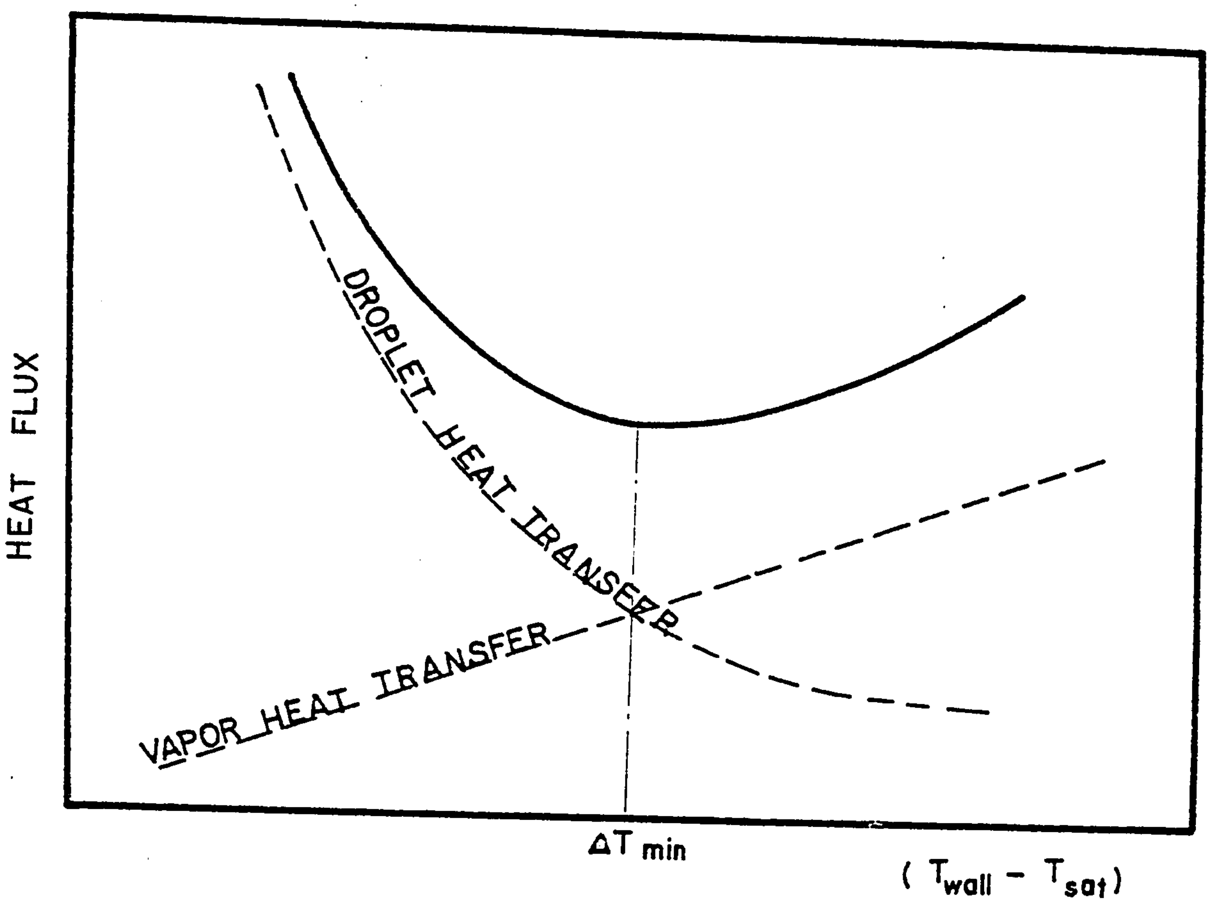

FIG.7 DISPERSED FLOW REWET

FROM ILOEJE, et al. [5]

each component with wall temperature.

Modelling the collapse in this manner reflects the effect of mass flux which was absent in the other two models. At high mass fluxes there is a greater mixing of the flow, and it therefore reduces superheating of the vapor, while it provides a greater momentum of droplets. All these factors will increase the heat transfer, and consequently lead to transition occurring at higher wall superheat. However, a difficulty exists in predicting the heat transfer component of the droplets.

1.2.5 - The Use of Electric Probes in Two-Phase Flow:

Electric probes can be used to measure the conductance, the capacitance and the rate of electric discharge. The most common and convenient electric probes are those of conductance type. So far, two methods for measuring the conductance of a flow regime are reported in the literature, i.e., i) Two-Electrode, and ii) Probe-to-Wall methods.

1.2.5.1 - Two-Electrode Method

G.F. Hewitt [12] used an electric probe-conductance type- to determine the average value of the film thickness in upwards annular flow of air water mixtures. The probes consisted of stainless steel rods passing through the tube wall and were made flush with the inner surface. The rods were 1/8" diameter and placed in line with 1/2" spacing between centres. Fig. 8 shows this arrangement along with a calibration cell. This set-up was used to obtain a plot of conductance between the probes against the film thickness of a solution of known conductivity. This technique was known as A.E.R.E method.

1.2.5.2 - Probe-to-Wall Method:

Through the use of an electric conductivity probe, Griffith [13,14] investigated the location of the transition between slug flow (liquid bridging) and annular flow (continuous gas core). His probe (Fig. 9) was used to determine the electrical resistance between the centre of the pipe and the wall.

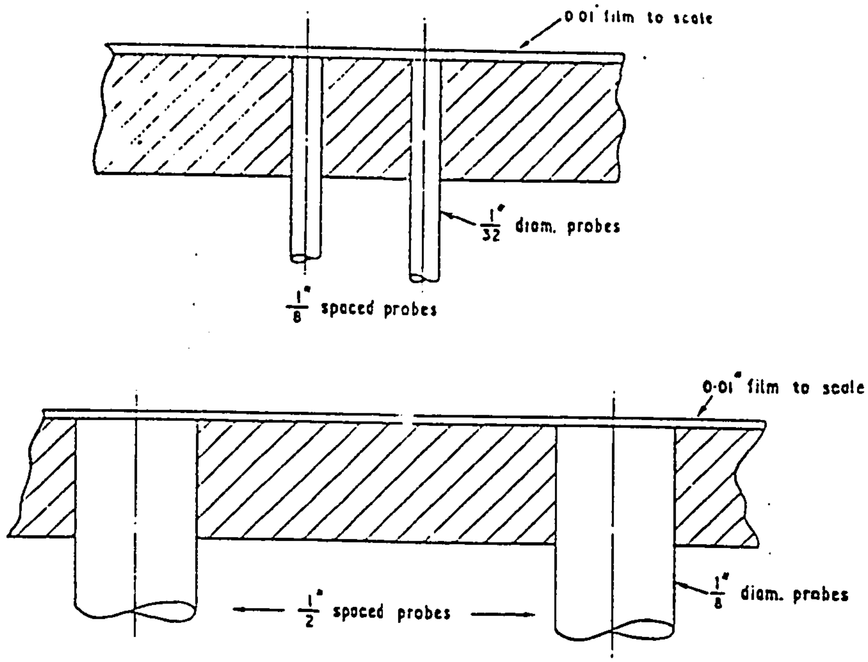

SCALE DRAWING OF 1/8" AND 1/2" SPACED PROBES COVERED BY 0·01" FILM.

A.E.RE.- R.3921.

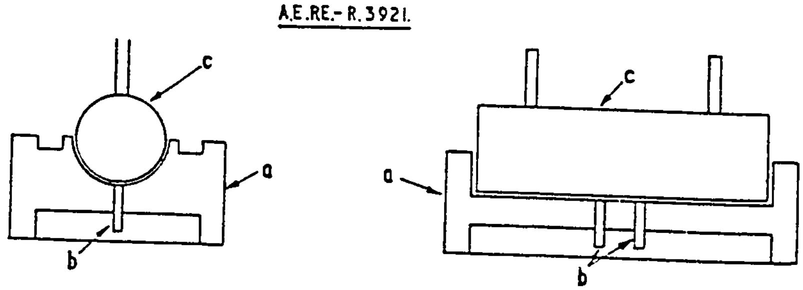

CONSTRUCTION OF FILM THICKN"SS CALIBRATION CELL.

A.E.R.E.- R.3921.

a- 1.250" Dia. perspex trough
b- Electrodes
c- 1.248" Dia. rod

FIG.8 TWO-ELECTRODE MEASUREMENTS

FROM HEWITT, et al. [12]

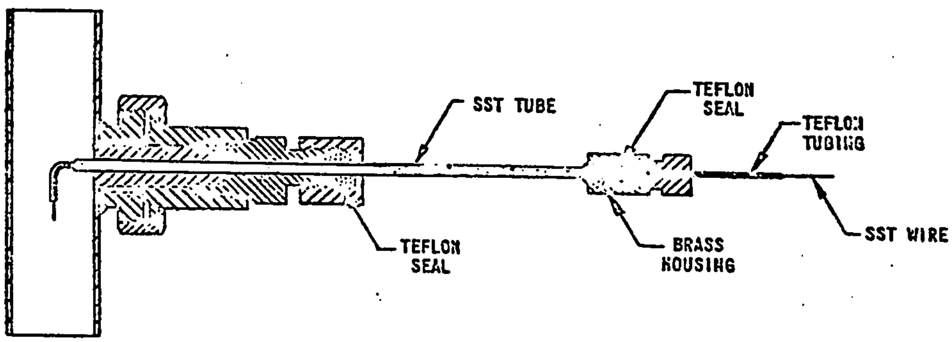

Probe Detail

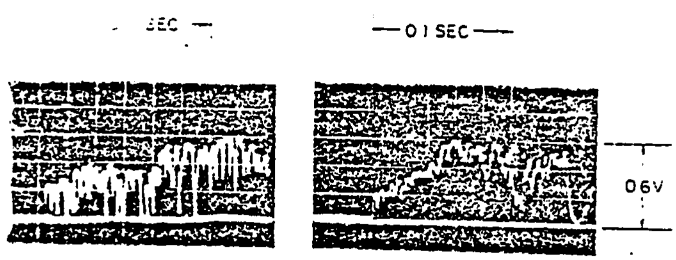

Typical slug-flow traces. Annular flow is simply a straight line on the lower axis

FIG. 9 PROBE-TO-WALL MEASUREMENTS

FROM GRIFFITH, [13,14]

The probe was to determine whether or not there were bridges of liquid across the channel.

Iida and Kobayasi [15] used an electric probe to study the behavior of vapor void in pool boiling, on a horizontal surface under atmospheric pressure. They measured the time variation of local vapor void by detecting the variation of the resistance as a voltage signal through the use of series resonance circuit. Fig. 10 shows the construction of the probe and the experimental apparatus along with the void signal. By using a three-dimensional micro-traveller, They could obtain void fraction distribution near the heating surface.

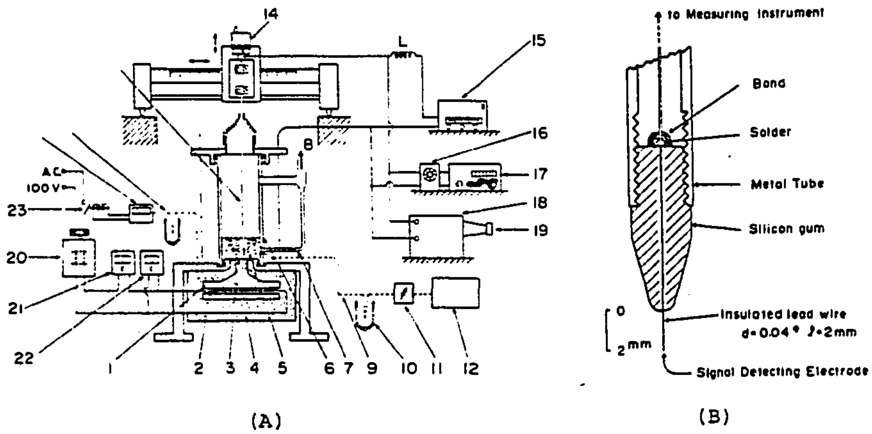

(A) Schematic diagram of experimental apparatus.
(B) Schema of the prove.

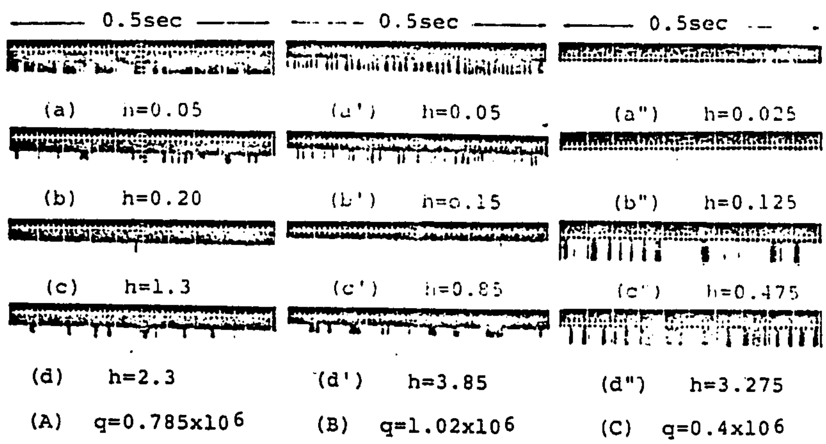

Typical examples of detected void signal in nucleate boiling (A),(B) and in film boiling (C). (q: kcal/m hr, h: mm)

FIG.10 PROBE-TO-WALL MEASUREMENTS

FROM IIDA [15]

CHAPTER 2

THE PROBES

Two types of electric probes are adopted for this study, a thermocouple probe and a Zirconium-Platinum probe.

2.1 - The Thermocouple Probe

2.1.1- Construction:

An ordinary K type of thermocouple was used to construct an electric probe. Fig. 11.a shows conductor wire positioned in compacted ceramic insulation (MgO) and surrounded by a tight fitting protective metal sheath. The measuring junction of the thermocouple was cut off first, then the original insulating material was removed to a depth of 1/8" (Fig. 11.b) and replaced by high temperature cement (Fig. 11.c). After the high temperature cement had set, the probe and surface were polished to avoid any spot which might have trapped bubbles during the test.

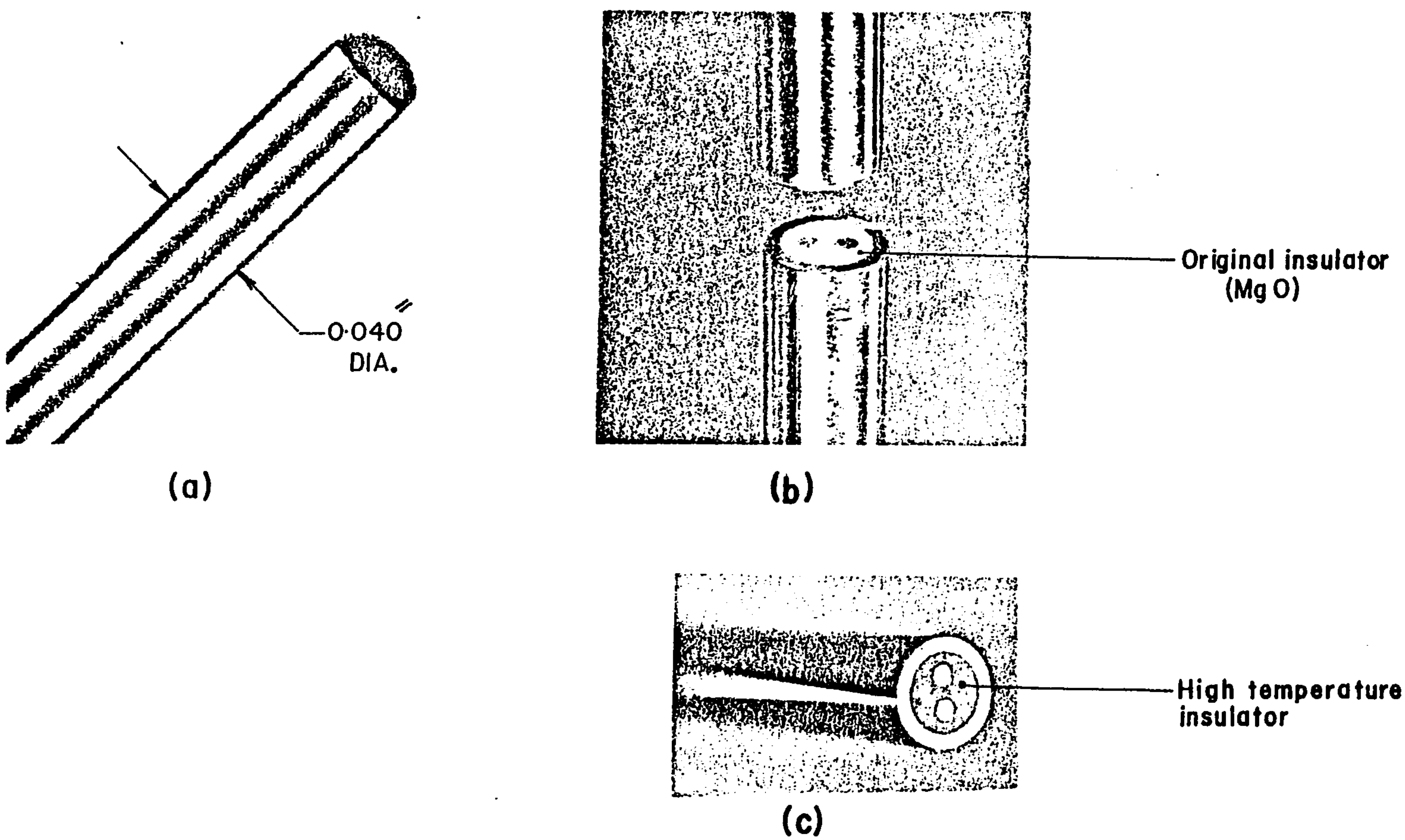

FIG.11 THE THERMOCOUPLE PROBE

2.1.2 - Probe Circuit:

Fig. 12 is a schematic diagram of the probe circuit which includes a 3V battery, a variable resistance and a chart recorder. The probe measures the electric resistance of flow phase on the wall. If the wall is dry, the resistance across AB is "infinite", therefore, a small voltage drop will be registered across CD. Similarly, if the wall is wet, the resistance is finite and a larger voltage drop across CD is noticed.

2.1.3 - Visual Experiment:

In order to relate visually, the output signals from the probe to the collapse of film boiling (rewetting) and the onset of nucleate boiling (max. heat flux), the probe was first tested in a pool boiling environment (Fig. 14). The test section, as shown in Fig. 13, consists of a copper cylinder heated by cartridge heaters and a probe inserted through the cylinder. For the purpose of prolonging the quenching time, only a small window of surface area around the probe was exposed and the

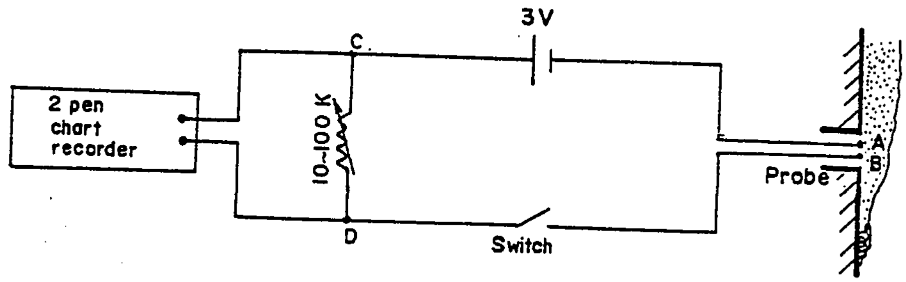

FIG. 12 PROBE CIRCUIT

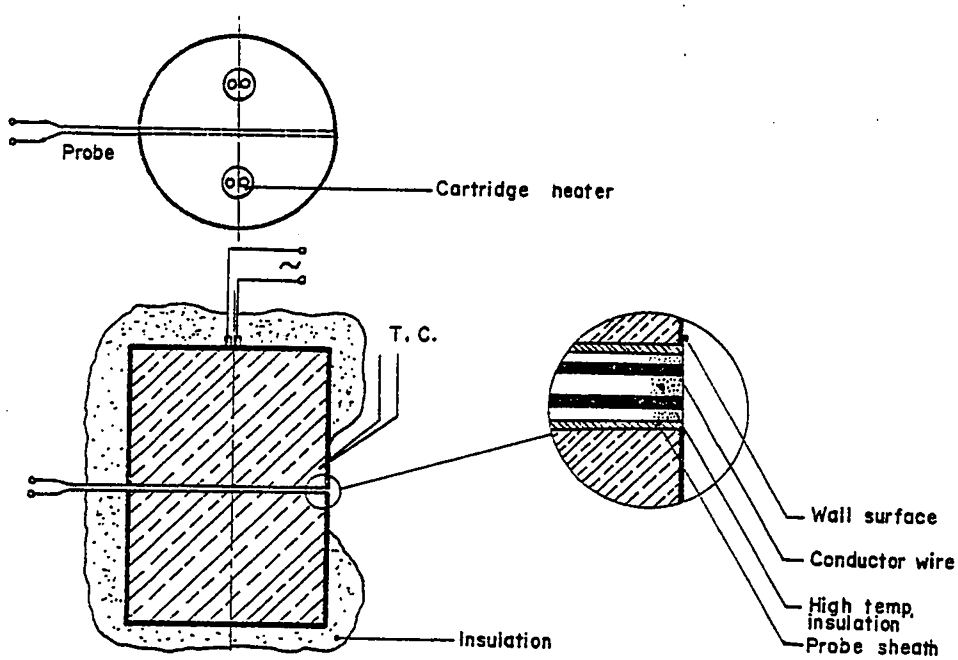

FIG. 13 TEST SECTION OF POOL BOILING EXPERIMET

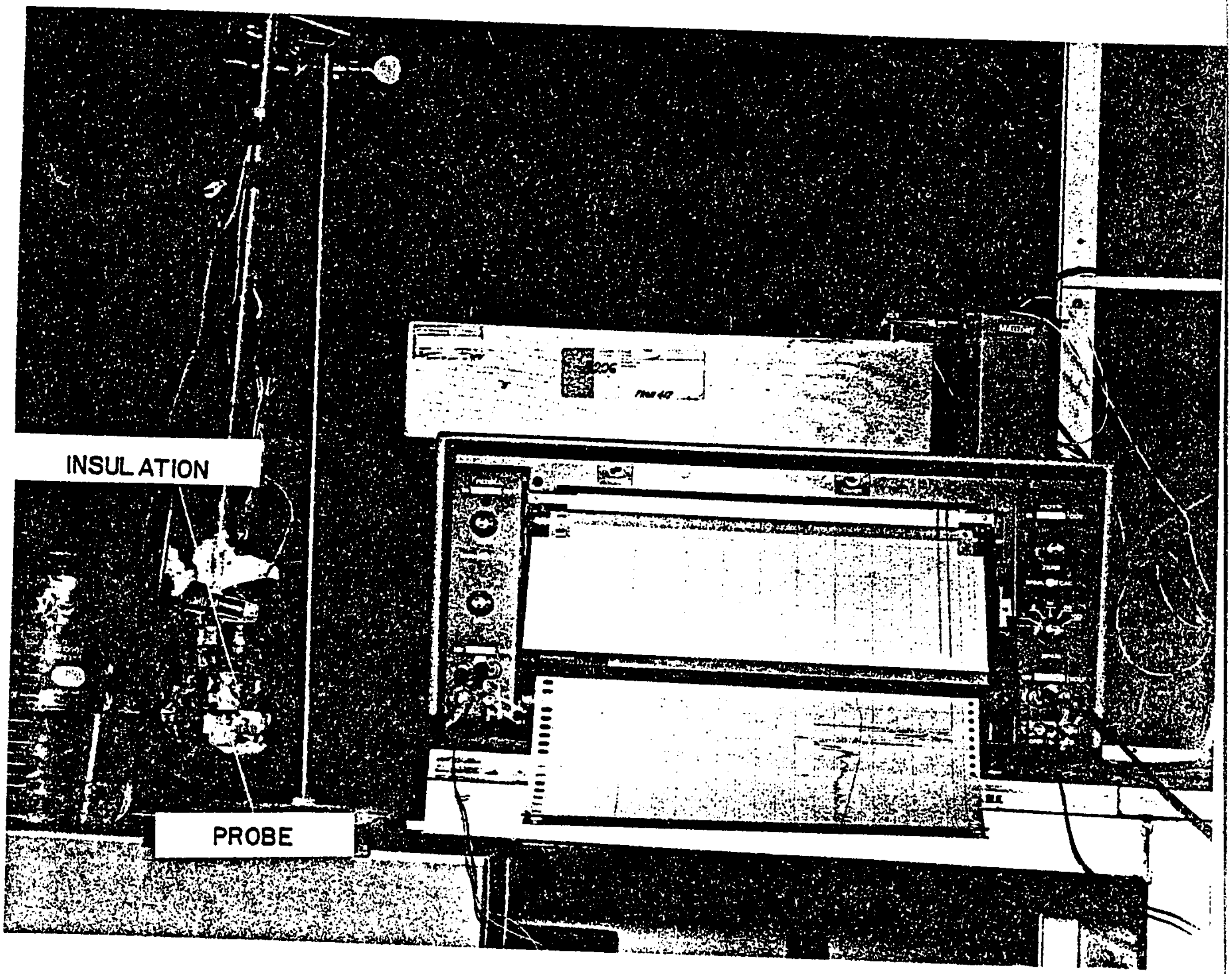

FIG.14 POOL BOILING EXPERIMENT

rest was insulated. To measure the wall temperature, a thermocouple was inserted in the test section very close to the probe. Temperature and probe traces were recorded simultaneously on a chart recorder.

2.1.4 - Signal Recorded from Thermocouple Probe in Pool Boiling:

Typical signal of the probe in pool boiling is presented in Fig. 15. The region AB in the probe trace represents film boiling, which was observed on the heated surface as a stable vapor film. When the film collapsed, the voltage rose suddenly from (B) to (C), characterizing the transition region. Beyond point (C), the nucleate boiling started and the voltage level stabilized at a higher value (C-D).

In some runs, it was impossible to obtain a stable vapor film at the start of the quenching process, due to the oxidation of the copper surface. When this occured, the test section had to be heated up to 600^{o}F to establish the film

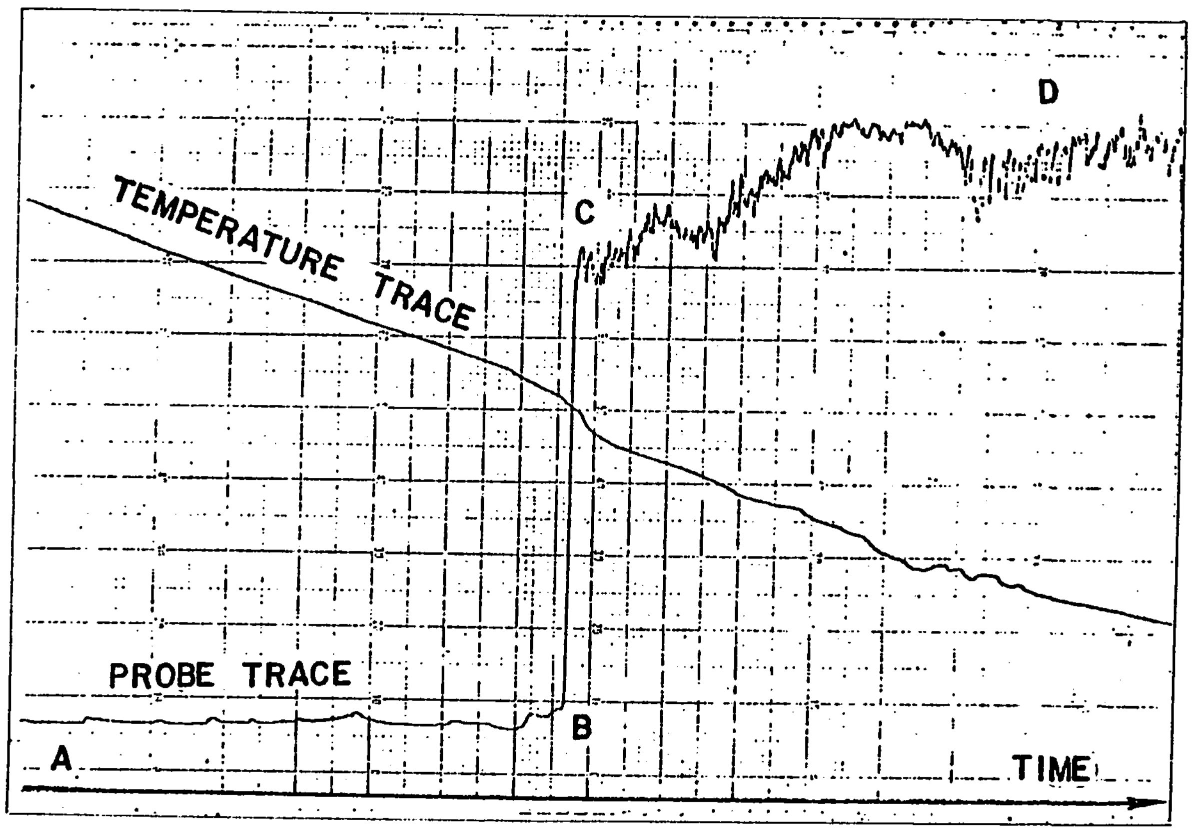

FIG.15 THERMOCOUPLE PROBE SIGNAL IN POOL BOILING

boiling regime. In this case, it was found that the collapse occured at a higher temperature. By polishing and cleaning the surface, using Carbon Tetrachloride, the vapor film could be re-established at approximately 450°F.

Some difficulties were experienced with the thermocouple probe during the experiments. High temperature cement between the two leads was washed away after a couple of runs, and vapor then became trapped in the probe cavity. The probe leads also oxidized, causing the probe to lose its sensitivity. When this happened, the probe tip was cut off, the original insulating material replaced by high temperature cement, and the probe tip repolished.

2.2 - The Zirconium-Platinum Probe

The difficulties experienced with the thermocouple probe led to the design of another type of electric probe that could withstand water conditions and corrosion. It was found that the zirconia (zirconium oxide) has been relied upon to prevent corrosion of the CANDU fuel. For this reason, a zirconium wire (0.040 DIA) was used to construct the electric probe shown in Fig. 16. To provide adequate insulation, the wire was coated with zirconia, which can be formed on the surface by autoclaving. The tip of the probe was made from platinum which was applied to the zirconium wire by sputtering process under vacuum conditions.

In the current arrangement, the platinum tip of the probe and the heating surface are used as two electrodes (Probe-to-Wall method). An alternative arrangement, using the same method, is suggested in Chapter 5.

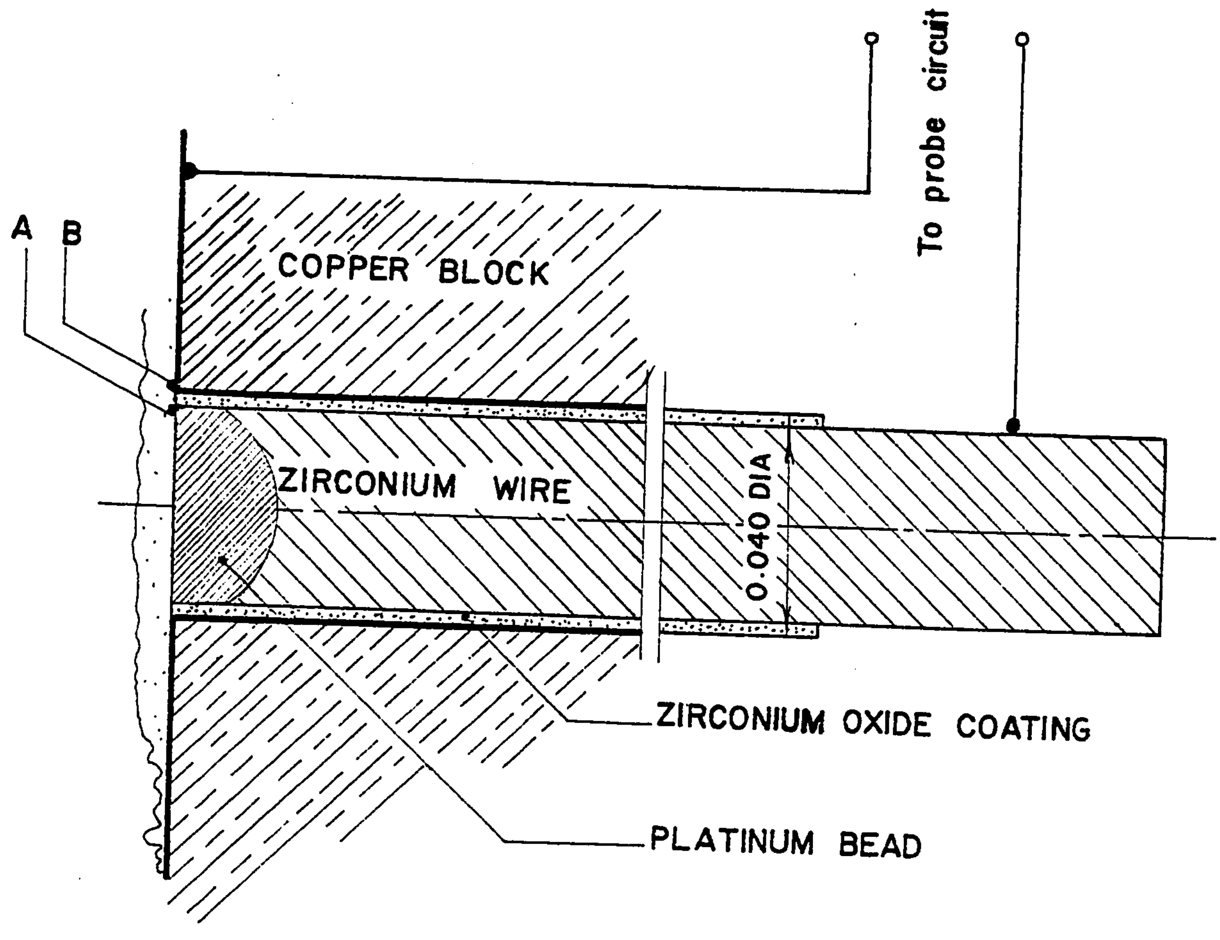

FIG. 16 THE ZIRCONIUM-PLATINUM PROBE

CHAPTER 3

EXPERIMENTAL APPARATUS AND PROCEDURES

3.1 - Description of Apparatus:

Fig. 17 is a schematic flow diagram showing the essential components of the test loop. These include a hot-water tank, pump, flow meter, test section, and the associated valves and piping. A general view of test apparatus is also shown in Fig. 18.

The hot water tank is powered by a 3kw immersion heater drawing current via a thermostat that can be adjusted to the desired inlet temperature. The water is circulated by 1/20 HP centrifugal pump and drained back to the tank. Pipings of the whole set-up are 1/2" copper pipe and are joined by soldering. The flow rate is measured and adjusted by a rotameter (0.48 G.P.M. max. capacity). Water temperature in the tank is measured by a thermocouple placed at the tank outlet. For accurate determination of water inlet subcooling, another thermocouple is

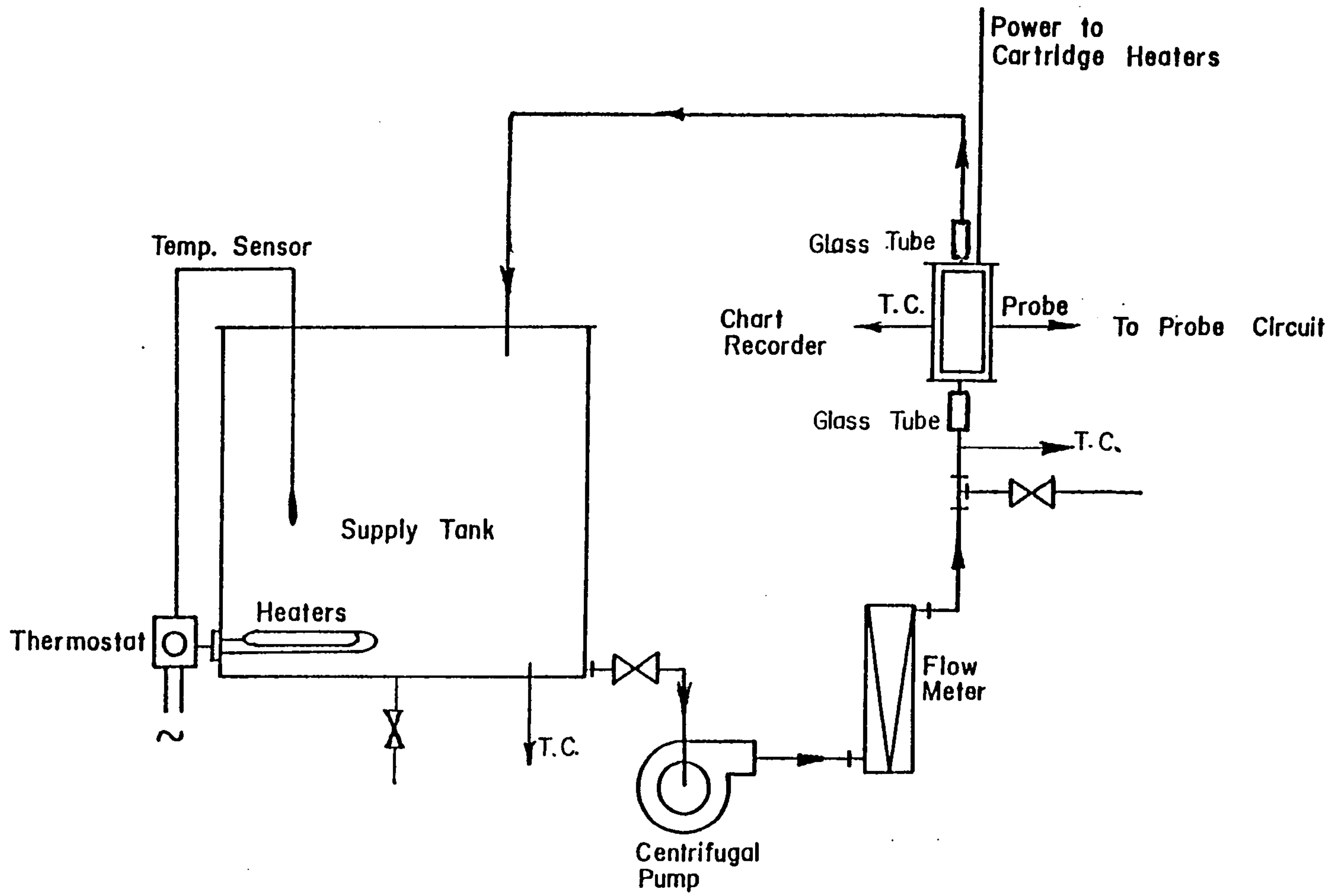

FIG.17 SCHEMATIC DIAGRAM OF FLOW LOOP

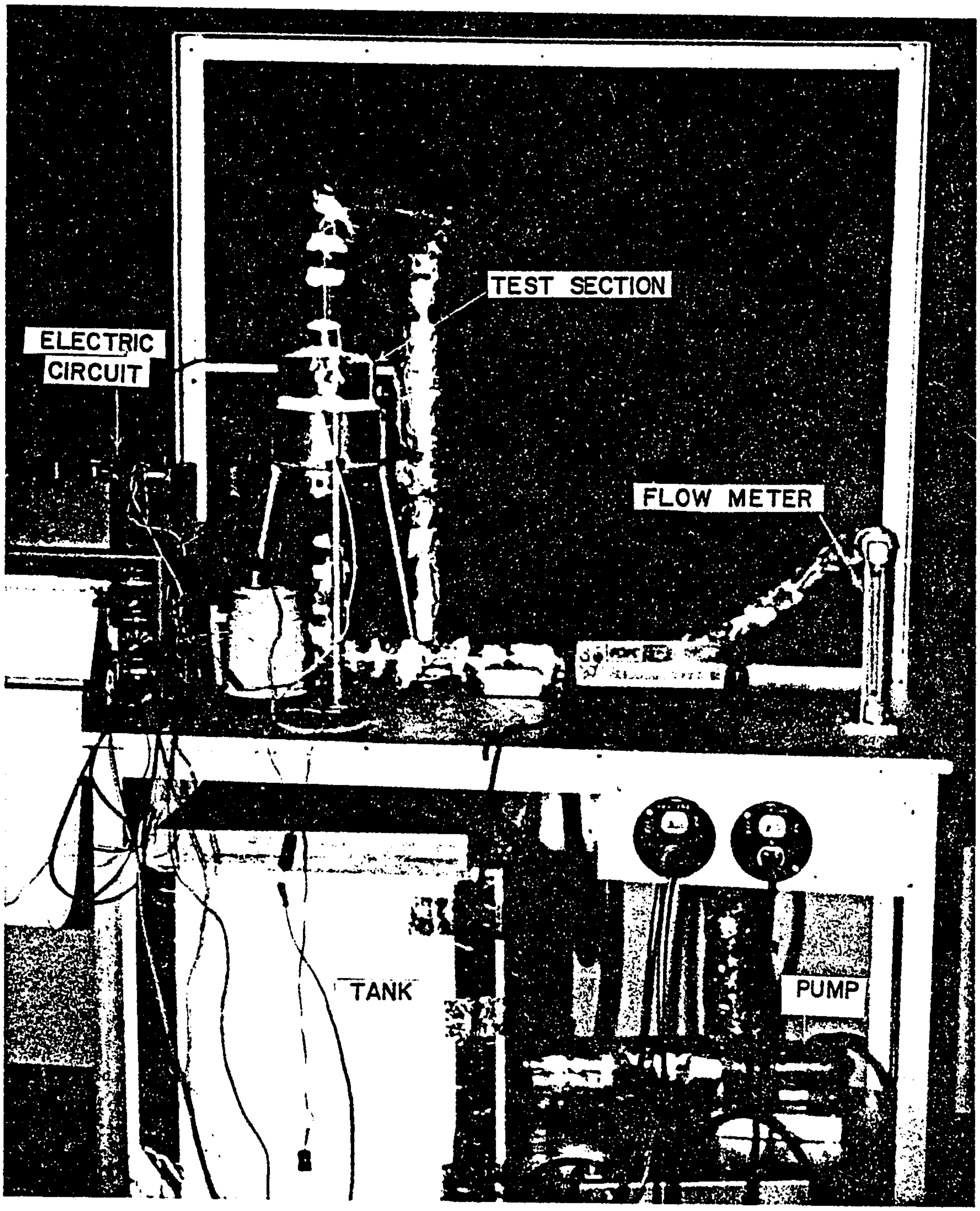

FIG.18 FLOW BOILING APPARATUS

placed near the inlet of the test section.

3.2 - Test Section:

The test section assembly, as shown in Fig. 19, consists of a copper block and two end fittings. Physical dimensions of the test section along with the thermocouple and probe locations are given in Figs 20,21,22. A centre bore of 1/2" is drilled in the copper block to allow the flow to pass through. The test section is insulated by FIBERFAX insulation. Heating of the test section is accomplished by using two cartridge heaters [1/4"D, 300 W].

In order to check and adjust the probe tip location on the inside surface, the test section has to be removed and installed frequently. For this reason, a simple design is chosen for mounting the test section. Inlet and outlet test sections are connected by means of two stainless steel unions to two glass tubes. The glass tubes will reduce heat losses to piping and permit flow visualization.

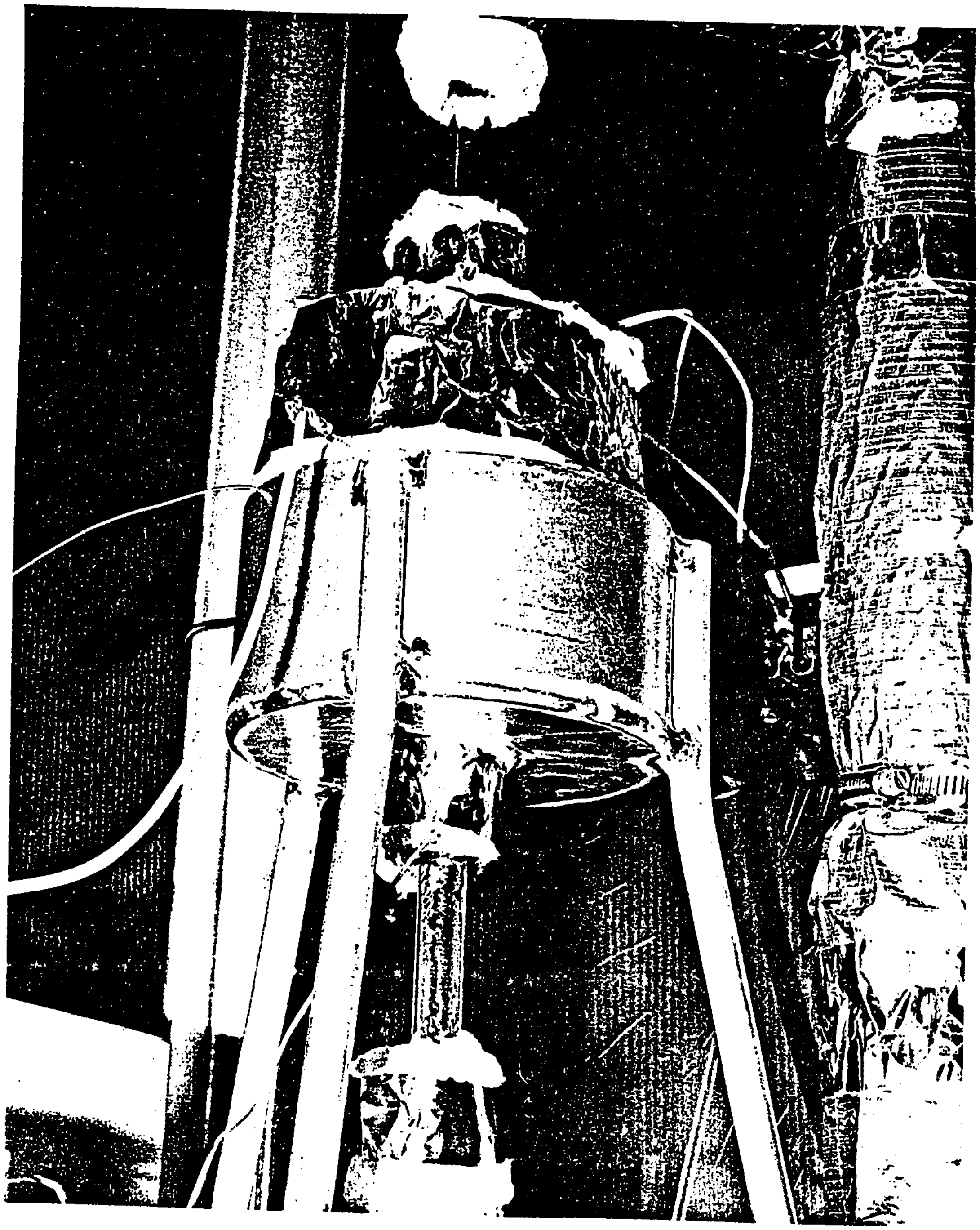

FIG. 19 TEST SECTION ASSEMBLY

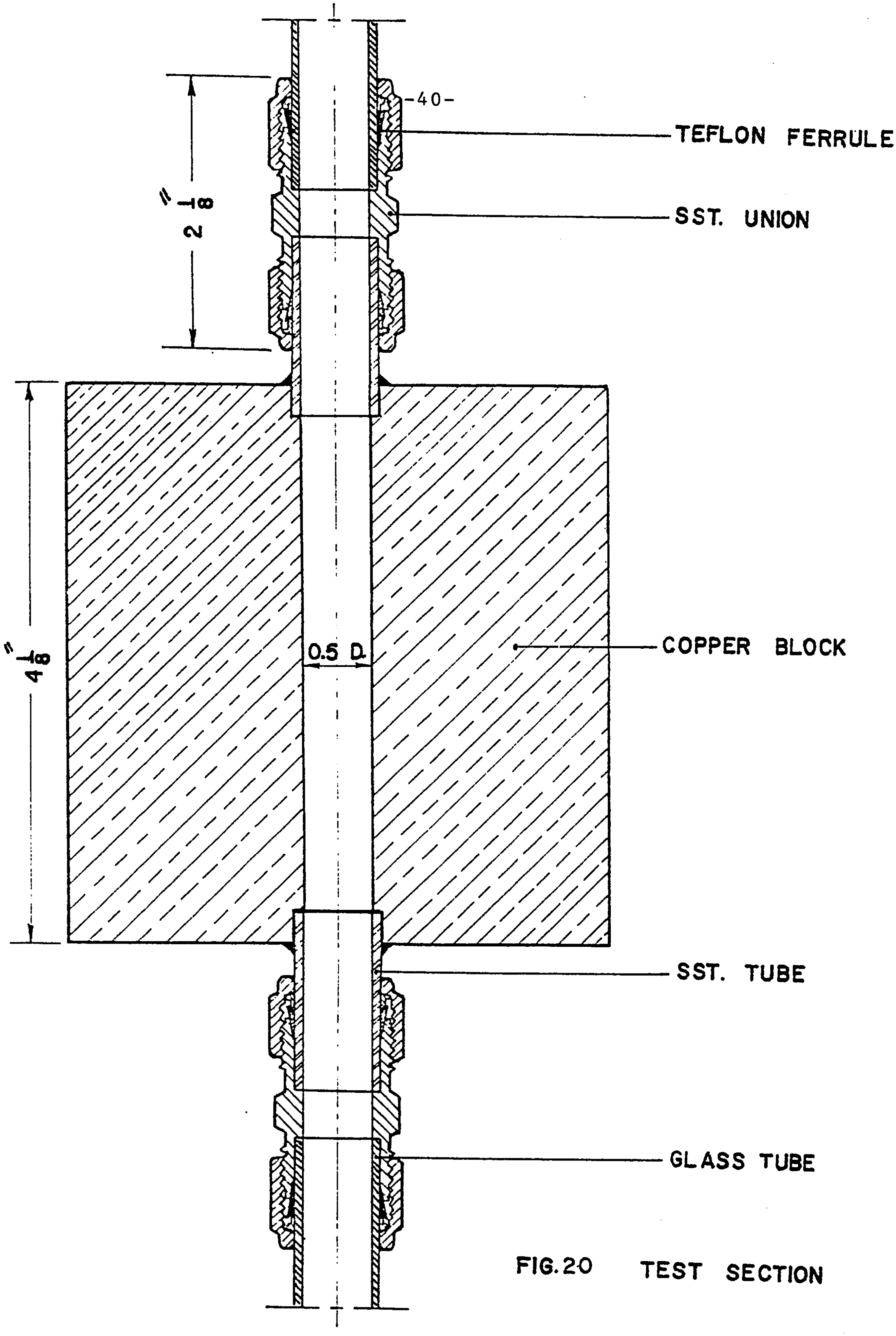

FIG. 20 TEST SECTION

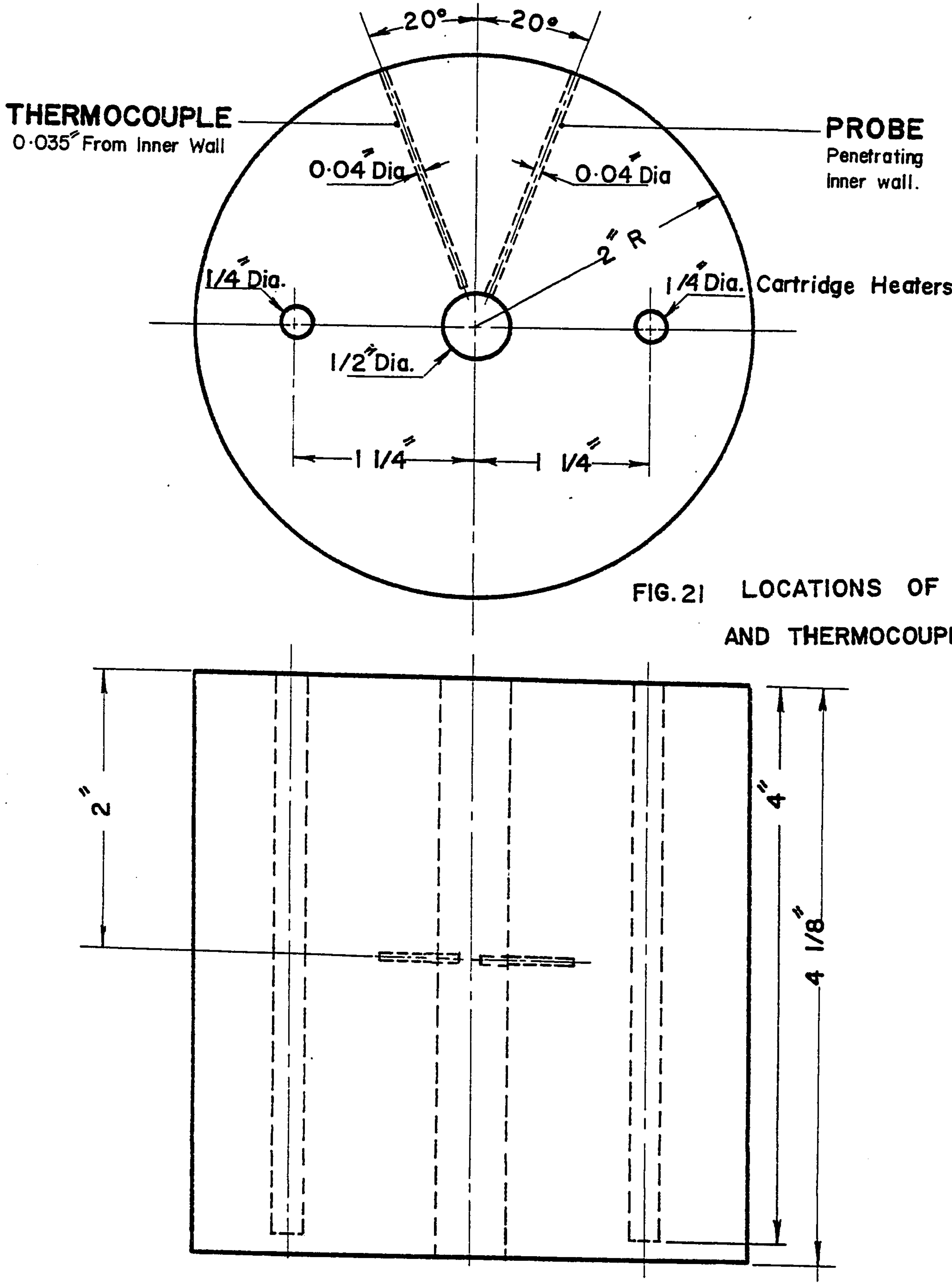

FIG. 21 LOCATIONS OF PROBE AND THERMOCOUPLE

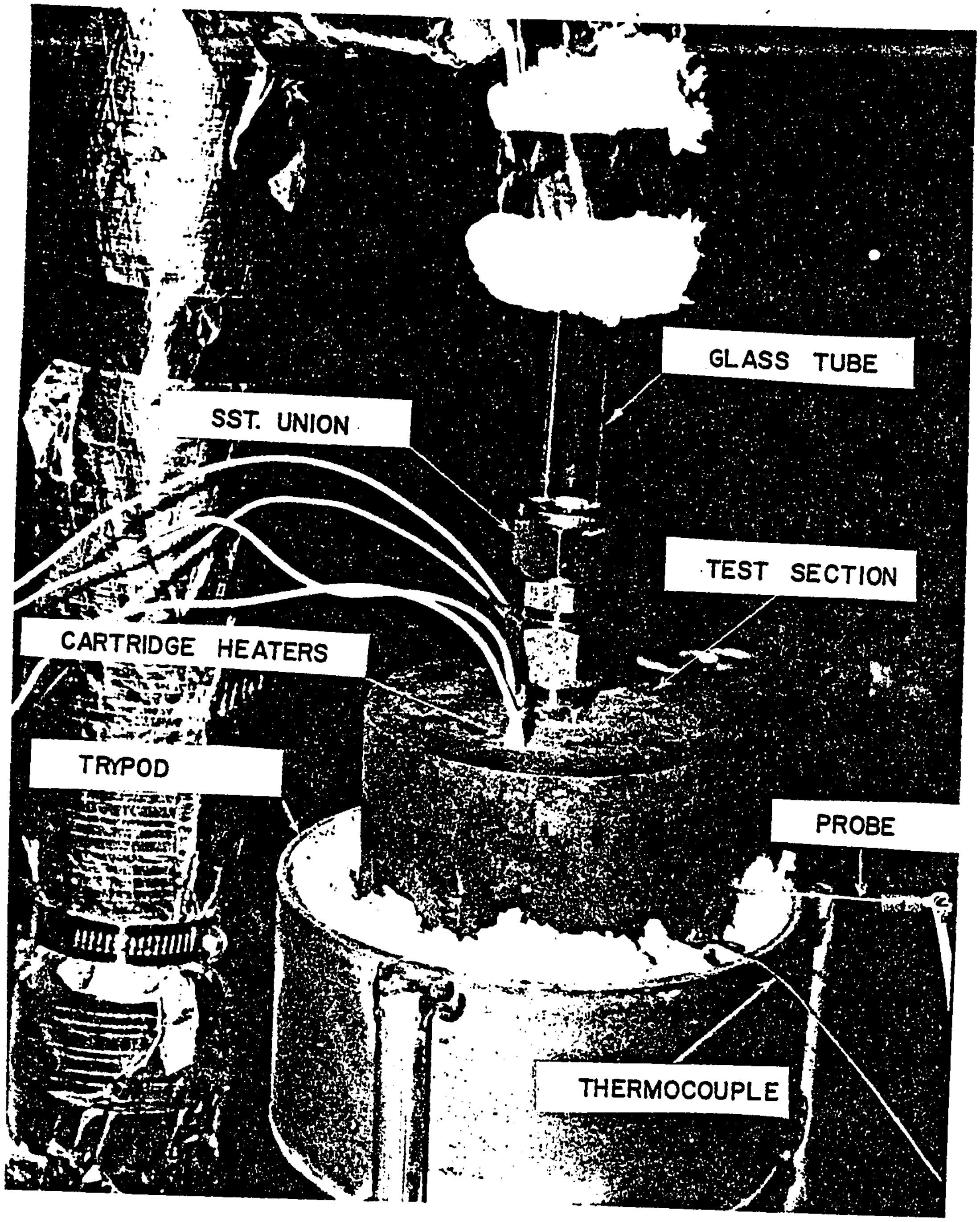

FIG.22 DETAILS OF THE TEST SECTION

3.3 - Experimental Procedures:

1 - Water in the storage tank is first heated to the desired temperature by an immersion heater which is thermostatically controlled. By means of a thermocouple, the approximate initially desired value is obtained.

2 - Lower and upper voltage levels of the probe output signal are checked by chart recorder. Low voltage level representing air resistance is determined under no-flow conditions. By passing the flow in the test section for a few seconds, voltage level representing water resistance is registered. A suitable span is chosen to incorporate these two points.

3 - Pump is turned on for circulation and adjustment of the flow rate. The flow is drained back to the storage tank.

4 - Test section is heated to the desired temperature.

5 - At the start of the quenching test, the cartridge heaters are turned off. After a short period (60 seconds), the flow is diverted to the test section by closing the drain valve. This delay period prior to the introduction of the flow, will allow a more uniform temperature distribution in the test section.

6 - Chart recorder is already running at the beginning of every test run.

CHAPTER 4

EXPERIMENTAL RUNS AND DATA REDUCTION

4.1 - General

Experimental runs consist of two test series; they are:

1. P200 series (Run Nos. *P200-P299) using the thermocouple probe described in Fig. 11.

2. P300 series (Run Nos. P300-P399) using the zirconium-platinum probe described in Fig. 16. (The P100 series numbers have been reserved for a preliminary test section reported in reference [16]).

---

*Letter 'P' which appears before a run number designates for the use of a 'Probe'.

In each series, runs were conducted for two different mass fluxes (0.25×10^5 and $0.5 \times 10^5 \, lbm/hr.ft^2$) and different degrees of subcooling. In every run, readings of the thermocouple and the electric probe were recorded simultaneously on a two channel chart recorder, running at a speed of 10 sec./in.

The probe trace, through one channel, provided information about different flow phases existing on the wall. From its trace, one could detect the start and end of vapor film collapse. The thermocouple trace, through the other channel, gave the temperature-time history, from which the boiling curve could be constructed. Since both traces were recorded simultaneously, changes of the flow phase could be related to heat transfer modes on the boiling curve.

4.2 - Signals Recorded from the Thermocouple Probe:

Using the same circuit of Fig. 12, the probe output was obtained under flow boiling conditions during a quenching process. A typical probe trace, along with thermocouple trace, obtained in run No. P203, are presented in Fig. 23.

Based on the probe trace, some general observations can be made:

i) Fluctuations in the film boiling region (A - B), as will be discussed later in 5.1, appear to be due to the effect of mass flux which was absent in the pool boiling experiment (see Fig. 15).

ii) The mean value of voltage fluctuations, represents the phase resistance on the wall defined as time average. This value is shown to be slightly higher than the voltage level (0 - A) representing the air before introducing the flow.

iii) In region (B - C), the voltage level rises drastically, indicating transition from film to nucleate boiling. During this period, flow oscillations in test section were observed from the glass tube, where slugs of vapor were seen to force the flow toward both up-and-down-stream directions.

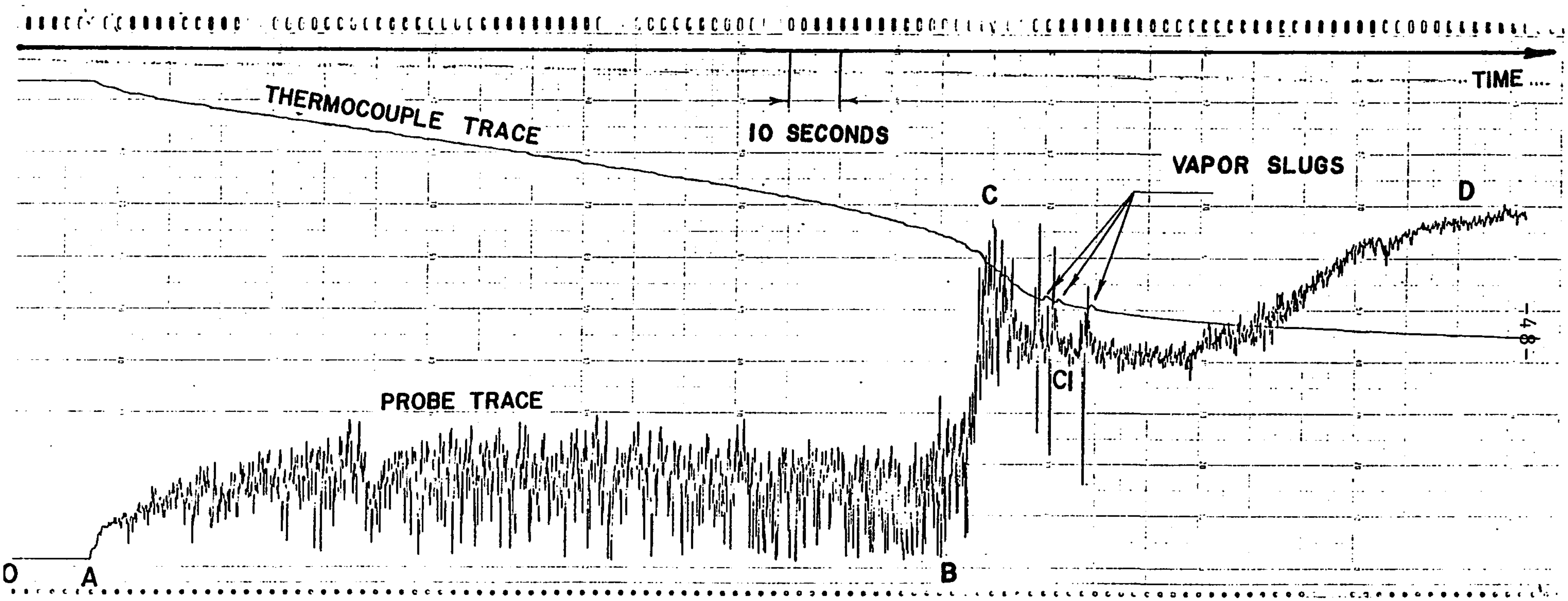

FIG. 23 SIGNAL RECORDED FROM THERMOCOUPLE PROBE IN FLOW BOILING

During the oscillations, flow meter readings fluctuated, at the same time, the thermocouple located near the inlet of the test section, picked up the temperature of vapor slugs instead of subcooled liquid.

iv) Beyond point (C), the voltage starts to stabilize at a value indicating the onset of stable nucleate boiling. At this stage, the slug flow was seen through upper glass tube, as shown in Fig. 24.

According to the above observations, the start and end of the collapse of vapor film were chosen as points (B) and (C) respectively. These points were then marked on the corresponding boiling curves.

4.3 - Signals Recorded from the Zirconium-Platinum Probe

Fig. 25 shows a typical signal recorded from the zirconium-platinum probe. Some observations based on this signal can be made in the following:

1. Fluctuations in film region AB are very

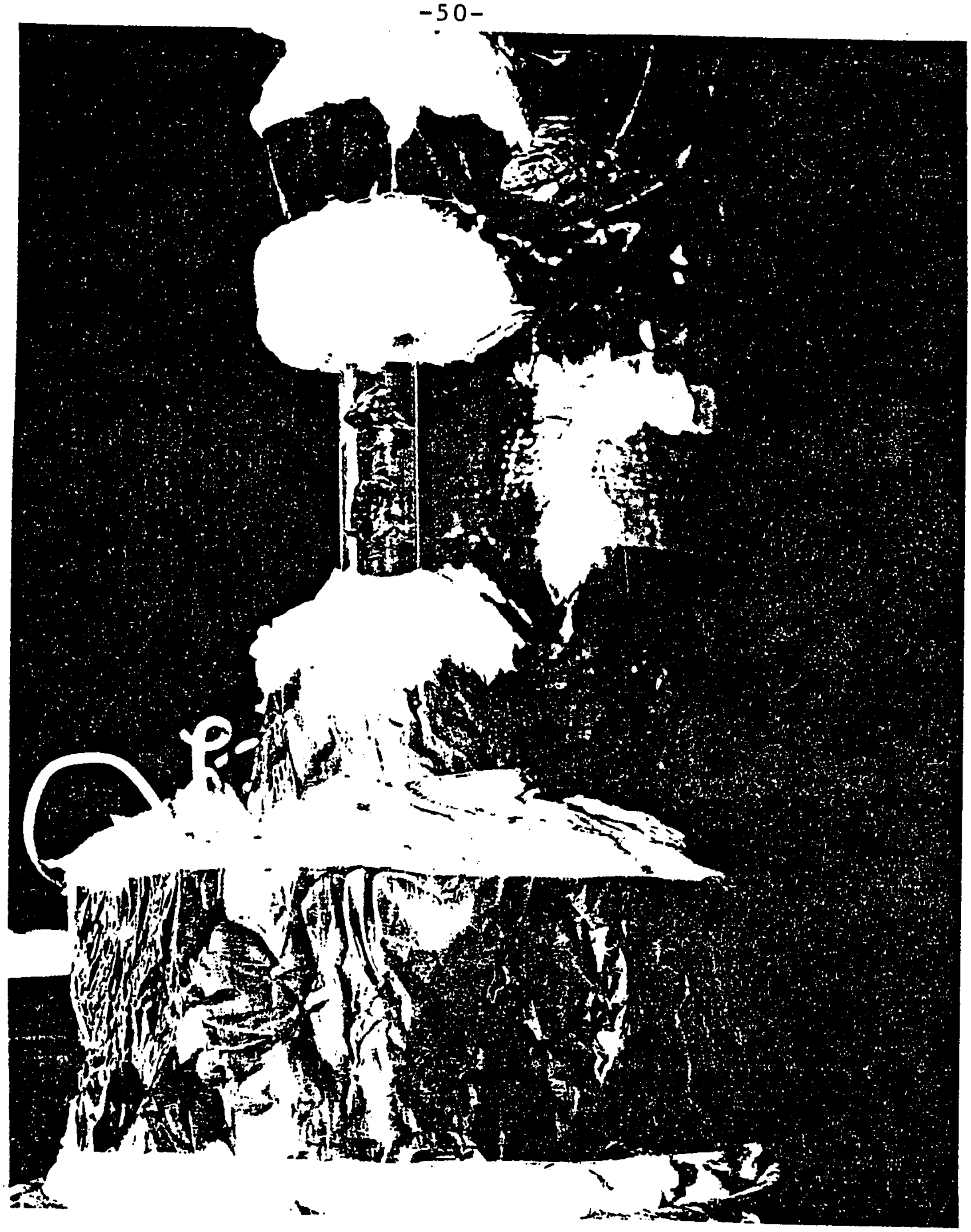

FIG.24 TYPICAL FLOW REGIMES IN BOILING TWO-PHASE FLOW OBSERVED THROUGH UPPER GLASS TUBE

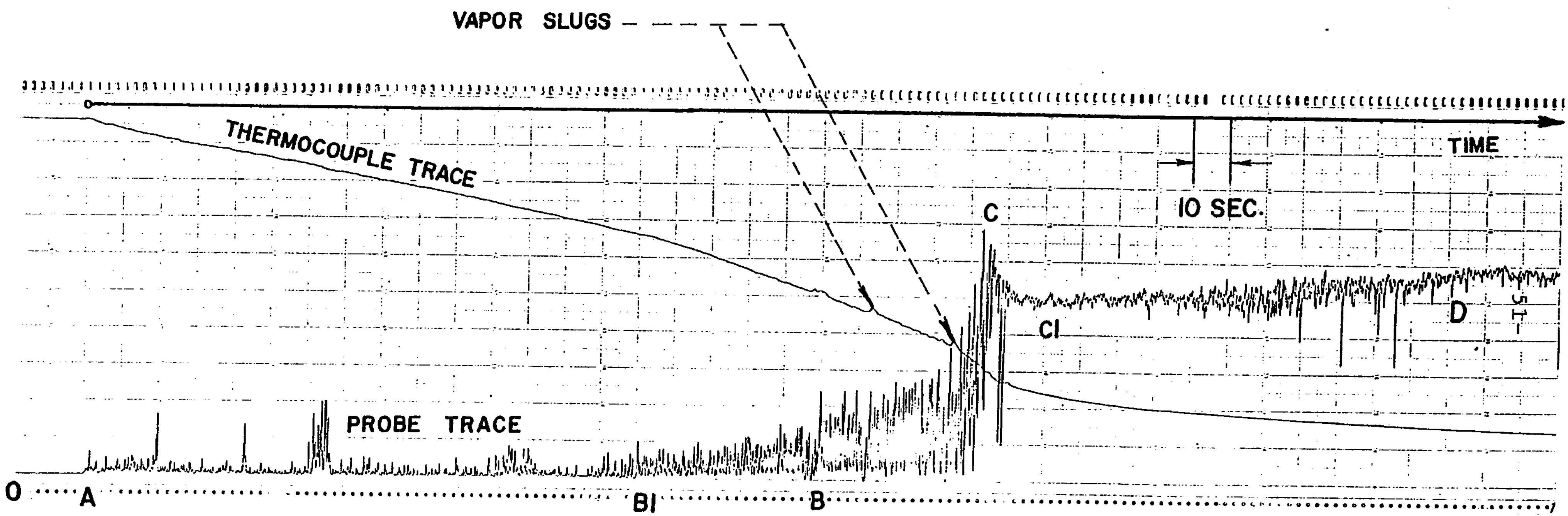

FIG.25 SIGNAL RECORDED FROM ZIRCONIUM-PLATINUM PROBE IN FLOW BOILING

small and mean electrical resistance measured is very high, indicating less liquid contact with the wall. This is believed to be due to the use of the wall as an electrode (Probe-to Wall measurement).

2. A local rewet appears in region B1.B, followed by a sudden rise in the voltage, from B to C, characterizing the transition from film to nucleate boiling. In this region, oscillations were observed through the glass tubes.

3. In region CD, the voltage stabilized at an approximately constant value representing the nucleate boiling region.

4.4 - Construction of Boiling Curves:

In order to obtain the boiling curves (heat flux-vs. wall temperature) from the temperature history as recorded from a thermocouple located near the wall, one has to solve the so-called inverse heat transfer problem. The inverse problem is one for which internal boundary conditions are described and the desired quantity is a surface condition (heat flux or wall temperature). This type of problem could be solved using the method of Burggraf [17], who obtained an exact solution in the form of rapidly convergent series. This solution involves the determination of third order derivative of T_o.

In this thesis, the mathematical model and computational technique developed by Cheng, et al. [18], is used to construct boiling curves. This method involves the calculation of heat flux by solving the Fourier transient equation and using the concept of rate of change of heat content within the test section.

For a hollow cylinder test section (Fig. 21) insulated on outer surface and both ends, heat transfer from the test section to the fluid between time 0 to t is assumed equal to the change in heat content Q inside the cylinder minus heat loss through the outer wall during the same time interval. Q can be expressed as:

$$Q(t) = \rho c_p L \int_{r_{in}}^{r_{out}} 2\pi r T dr \qquad (4.1)$$

where L represents the length of the test section. The function $T(r,t)$ is obtained as the solution to the one-dimensional Fourier equation in cylindrical coordinates:

$$\frac{\partial T}{\partial t} = \alpha\left(\frac{\partial^2 T}{\partial r^2} + \frac{1}{r}\frac{\partial T}{\partial r} \right) \qquad (4.2)$$

and is subject to the following initial and boundary conditions:

(1) $T = T(r,0)$ ... In general, at $t = 0$, (4.3)
the temperature across the test section is linear with about $8^{o}F$ difference.

(2) $T(r_o,t) = T_o$ ... r_o and T_o are the location and recordings of T.C., respectively. (4.4)

(3) $-k \left.\frac{\partial T}{\partial r}\right)_{r=r_{out}} = h(T_n - T_{amb})$ ... h is the heat (4.5)

transfer coefficient at the outer wall and its determination will be explained later.

The solution of Eq. (4.2) can be obtained by reducing it to a system of linear first-order differential equations in t. This is achieved by discretizing along the r-direction (Fig. 26), using the approximation:

$$\left.\frac{\partial T}{\partial r}\right|_{r=r_i} = \frac{T_{i+1}(t) - T_{i-1}(t)}{2\Delta r} \tag{4.6}$$

and

$$\left.\frac{\partial^2 T}{\partial r^2}\right|_{r=r_i} = \frac{T_{i-1}(t) - 2T_i(t) + T_{i+1}(t)}{(\Delta r)^2} \tag{4.7}$$

where $T_i(t)$ represents the temperature at the ith nodal point

$$(1 \leq i \leq n + 1) \quad \text{and} \quad \Delta r = \left[r_{out} - (r_{in} + \Delta r_o)\right]/n.$$

Using Eqs. (4.6) and (4.7) along with initial and boundary conditions, the following system of equations can be inferred from Eq. (4.2),

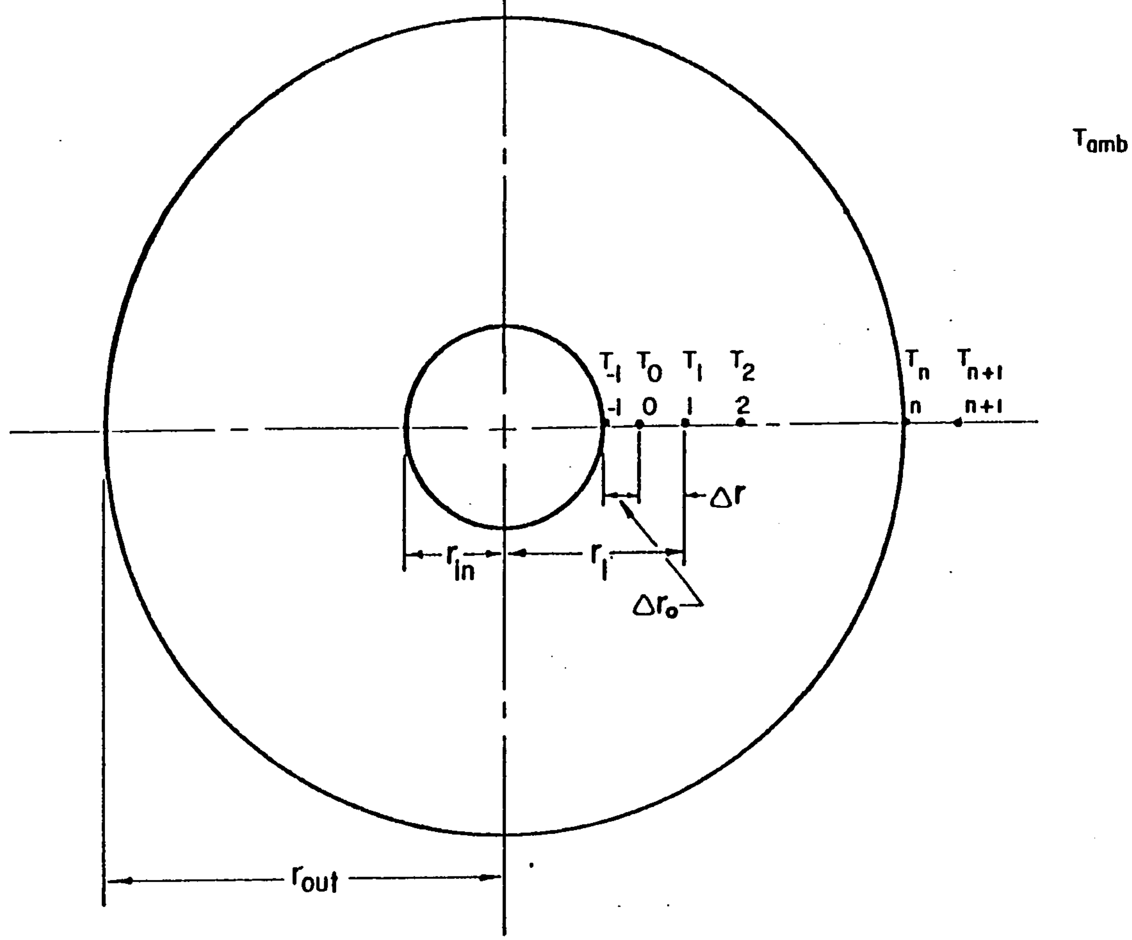

FIG. 26 NODAL POINTS DISTRIBUTION

$$\frac{dT_i}{dt} = \alpha \left[\frac{T_{i-1} - 2T_i + T_{i+1}}{(\Delta r)^2}\right] + \frac{\alpha}{r_i} \left(\frac{T_{i+1} - T_{i-1}}{2\Delta r} \right) \qquad (4.8)$$

$$1 \leq i \leq n$$

where $r_i = r_{in} + \Delta r_o + i\Delta r$

and

$$-\frac{k}{2} \left(\frac{T_n - T_{n-1}}{\Delta r} + \frac{T_{n+1} - T_n}{\Delta r} \right) = h(T_n - T_{amb}) \qquad (4.9)$$

Eq. (4.9) is a direct consequence of Eq. (4.5). Furthermore, T_{n+1} in Eq. (4.8) can be eliminated by using Eq. (4.9).

Eq. (4.8) contains a system of n equations with n unknowns in T_i and are readily solved. Once T_1 up to T_n have been solved and dT_o/dt determined experimentally, the inner wall temperature T_{-1} can then be calculated in the following Fourier equation based on the nodal point $i=0$

$$\frac{dT_o}{dt} = \alpha \frac{\frac{T_1 - T_o}{\Delta r} - \frac{T_o - T_{-1}}{\Delta r_o}}{\frac{1}{2}(\Delta r + \Delta r_o)} + \frac{\alpha}{r_o} \left(\frac{T_1 - T_{-1}}{\Delta r + \Delta r_o} \right) \qquad (4.10)$$

Eq. (4.1), expressed in terms of summation, becomes

$$Q = 2\pi\rho c_p L\left[0.5T_{-1}\, r_{in}\Delta r_o + 0.5T_o(r_{in} + \Delta r_o)\Delta r_o\right.$$

$$\left.+ 0.5T_o(r_{in} + \Delta r_o)\Delta r + (\sum_{j=1}^{n-1} T_j r_j + 0.5T_n r_n)\Delta r\right] \qquad (4.11)$$

The expression of net heat transfer to the fluid, q, in terms of Q and heat loss is:

$$q = -\frac{dQ}{dt}/A_{in} - hA_{out}\,(T_n - T_{amb})/A_{in}$$

$$= -\frac{1}{2\ r_{in}L}\frac{dQ}{dt} - \frac{hr_{out}}{r_{in}}(T_n - T_{amb}) \qquad (4.12)$$

where A_{in} and A_{out} represent the inner and the outer test section area, respectively.

All calculations are performed via CSMP computer package [19]. Due to its flexibility, power, relative ease of use and plotting capability, CSMP has gained wide acceptance recently in solving differential equations [20]. The Runge-Kutta fixed-step size method has been used in numerical integration with selection of n = 8 and $\Delta t = 0.1$ sec and its convergency checked. NLFGEN function generation (nonlinear function generation) capability of CSMP is used to generate T_o from experimental data and DERIV (derivative) module used to compute dT_o/dt from T_o and $\frac{dQ}{dt}$ from Q. A complete program has been established starting with T.C. recordings (millivolts vs time) as input, and at the end q vs the wall temperature printed and plotted (for a sample program, see Appendix). The conversion table for millivolts vs temperatures has been built in the program to expedite the conversion.

The heat transfer coefficient h at the outer wall of the test section has been determined experimentally under a no-flow condition*. Its value stays nearly constant at 6 Btu/hr-ft^2-^{o}F for most of the temperature range operated. For simplicity, a constant value of 6 Btu/hr-ft^2-^{o}F has been assumed in the computation. However, a variable expression of h as a function of temperature

---

* See reference [24] Appendices I and II for details of this experiment.

can be simply incorporated within CSMP capability by using the function generation.

The proposed method to construct a boiling curve from quenching data is only valid when no axial conduction exists. In reality, there is always some axial conduction occurring, e.g. imperfect insulation at the end of the test section. More severe axial heat loss could occur due to the possibility of nucleate boiling present just outside both ends of the test section and initiate rewetting fronts [7]. These rewetting fronts could then travel back into the test section, thus interfering with the spontaneous rewetting phenomenon inside the test section. However, in the present experimental set-up, the test section is connected to the piping by means of a thin-walled stainless steel tube, a stainless steel union and a glass tube. The relatively low conductivity and the thin wall of the stainless steel tube will minimize heat losses from the test section. Also, the glass tube will further reduce heat losses to the piping.

During the quenching process in the current study, the heaters are shut off. In order to prolong the quenching time, especially the duration of transition boiling time, the heaters could be left on. From the analysis point of view, this requires a modification of the Fourier equation by incorporating the proper heat source term.

CHAPTER 5

DISCUSSION OF RESULTS AND CONCLUSIONS

The present measuring technique not only detects rewetting and maximum heat flux points, but also provides some knowledge on boiling phenomena during a quenching process. Therefore, before making a comparison between the probe results and boiling curves, several observations based on the probe signal in different boiling regimes are discussed.

5.1 - Liquid-Solid Contact in Film Boiling Regime:

There has been considerable debate as to the existence of liquid-solid contact in stable film boiling regime. A physical evidence of the existence of such contacts was provided by the signals obtained from both types of probe in film boiling. As shown in Fig. 25 (region AB), fluctuations in probe trace indicate clearly the intermittent liquid hitting of the wall under forced vertical flow condition.

Since these fluctuations were absent in pool boiling experiment (see Fig. 15, region AB), it is reasonable to believe that the liquid hitting is due to the mass flux which causes greater mixing of the flow and greater momentum of the droplets. Liquid-solid contact can either be attained by droplets entrained in the vapor film, or by the wavy liquid-vapor interface, depending on the vapor film thickness and wall roughness.

The vapor film thickness has been measured, in pool boiling, by Iida, Y. [15]. He found that the thickness of the film layer over a flat copper surface is quite small, and less than 0.05 mm (< 0.002"). If this is true in pool boiling, it is then expected, with the introduction of the velocity component in flow boiling, that this thickness will be less and the liquid-solid contact becomes possible.

5.2 - Synchronized Recording of Vapor Slugs:

Vapor slugs formed on the wall were detected by the electric probe and thermocouple simultaneously. The thermocouple indicated a local wall temperature rise, while the probe gave a sudden drop in voltage. This synchronized recording is shown in Fig. 27.

Fiori and Bergles [21] reported a similar finding onF the effect of such slugs passing over a thermocouple through synchronized temperature recordings and photographs. Fig. 28 is the surface temperature trace, showing the dry spots and quenching slugs.

5.3 - Bubble Formation and Nucleation Density in Nucleate Boiling Region:

Beyond point C (Fig. 23,25), both types of probe showed an increase in phase resistance on the wall up to point C1, where it starts to decrease assymptotically. One likely explanation for this trend is that due to the onset of bubble formation* the contact area decreases, causing higher

---

*This should not be confused with the onset of nucleate boiling in heating an originally cold surface.

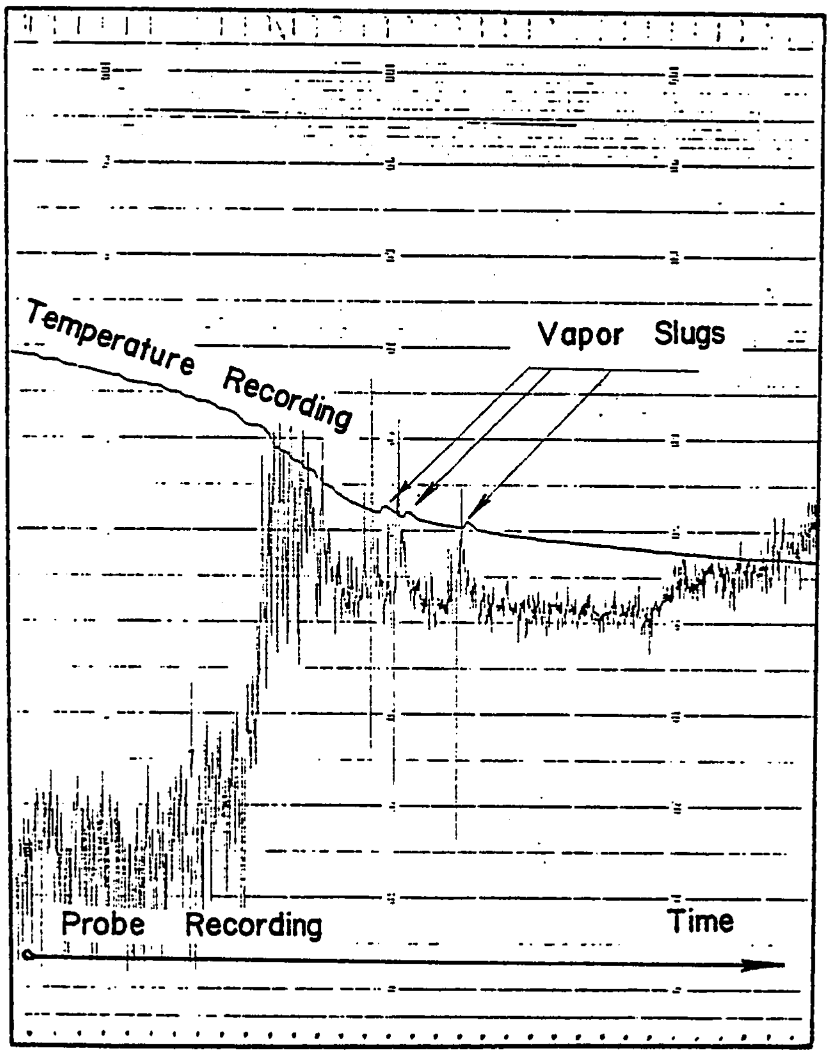

FIG. 27 SYNCHRONIZED RECORDINGS OF VAPOR SLUGS

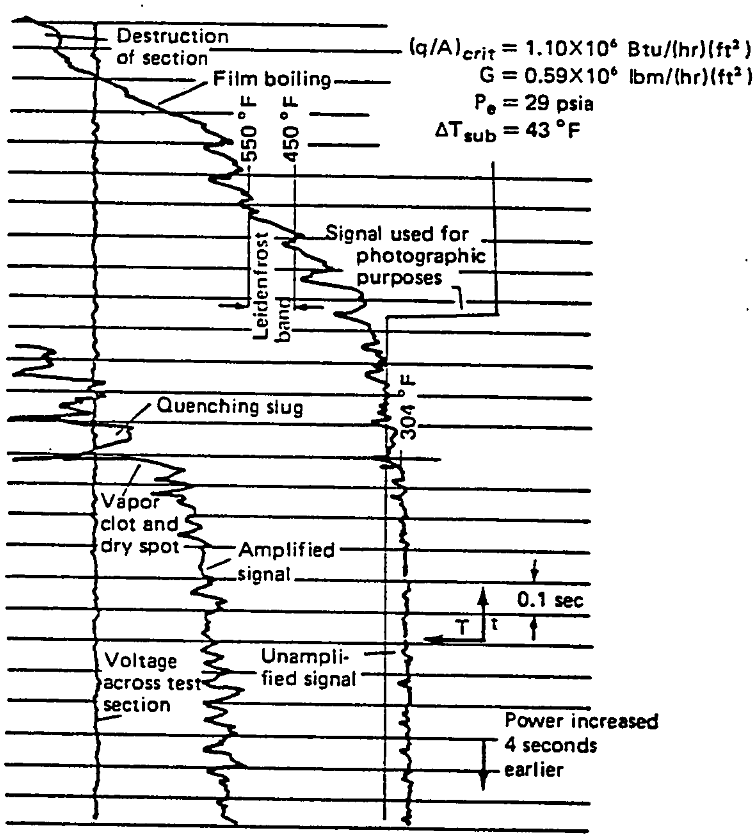

Surface temperature trace near the onset of burnout. (Fiori and Bergles)

FIG. 28 VAPOR SLUGS DETECTED BY THERMOCOUPLE

FROM HSU [25]

resistance on the wall. However, further decrease in surface temperature (from C1 to D), reduces bubble density and vapor void, causing lower resistance on the wall.

A similar trend was detected by Bradfield [22], when he measured the change in surface contact in quenching a chrome-plated copper cylinder. Fig. 30 shows his area ratio curve, where the nucleate boiling region is marked by the region of decreasing contact area.

It should be pointed out, however, that the nucleation density is not the only factor controlling the resistance on the wall during a nucleation process. In fact, the decrease of liquid temperature, during this process, causes an increase in the resistance on the wall, ie. producing an effect opposite to nucleation density. The sum of the two effects (nucleation density and liquid temperature) gives the total resistance measured by the probe. Since this total resistance, as recorded by the probe, continues to decrease (see

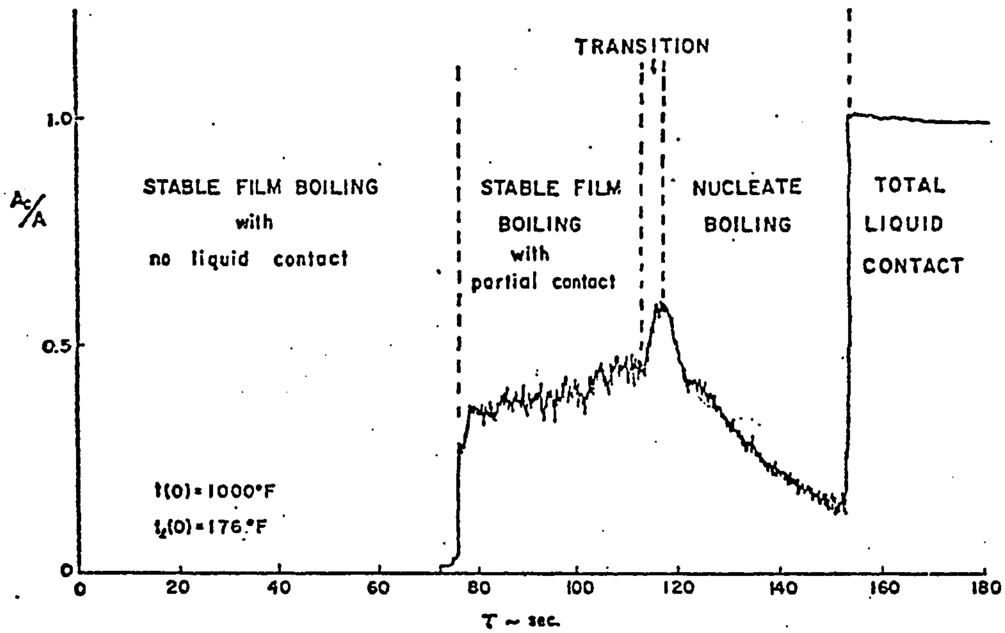

FIG. 29 PARTIAL LIQUID-SOLID CONTACT IN QUENCHING

FROM BRADFIELD [22]

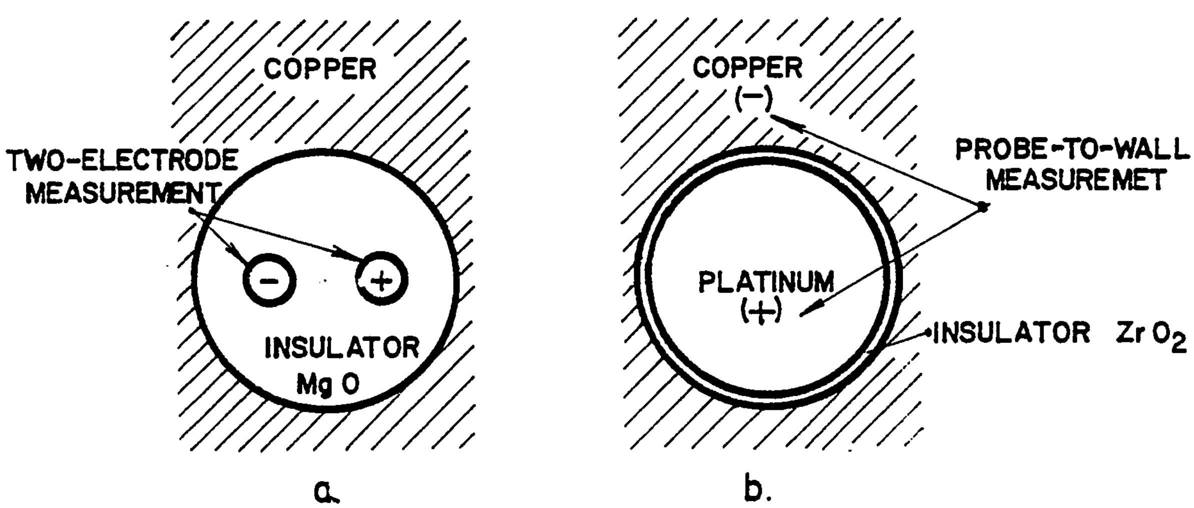

FIG.30 COMPARISON BETWEEN TWO METHODS OF MEASUREMENT

Fig. 25, region C1D), it can be concluded that the decrease in the resistance due to bubble density effect offsets the increase in the resistance caused by the temperature decrease.

5.4 - Advantages of Using Probe-to-Wall Measurement

Probe-to-Wall measurement showed very small fluctuations in the signal of film region AB (Fig. 25), indicating less liquid contact with the wall. This could be to the use of the wall as an electrode. In this case, resistance measured involves the flow in direct contact with the wall, which is vapor. In the two-electrode method, the two electrodes were surrounded by a ceramic material (MgO) whose thermal conductivity is much lower than the material of the wall. It is then possible for the ceramic surface of the probe to be at a much lower temperature than the copper wall, allowing local rewet on the probe tip while the wall is still blanketed by vapor.

Another possible explanation for the small fluctuations, is that the resistance is measured across a circumference of circle separating the two electrodes. A sketch of the conduction across this circumference, compared with the case of two-electrode-measurement, is given in Fig. 30. It can be seen from Fig. 30(a) that one droplet hitting the probe surface between the two electrodes, may be enough to provide large voltage rise. If, however, this droplet fell on the probe surface of Fig. 30(b) a slight voltage rise will be noticed, since only a few conduction lines are established between the two circular electrodes. Based on this fact, one may expect that the more liquid hitting of the probe, the higher is the output voltage, i.e. the output voltage will be proportional to the liquid-solid contact area. This feature may explain the gradual increase of such contacts detected by the zirconium-platinum probe in film boiling (see region B1.B) of Fig. 25.

5.5 - Rewetting and Maximum Heat Flux Points:

Results of the P200 series, using the thermocouple probe and the P300 series using the zirconium-platinum probe are presented in Figs. 31-34.

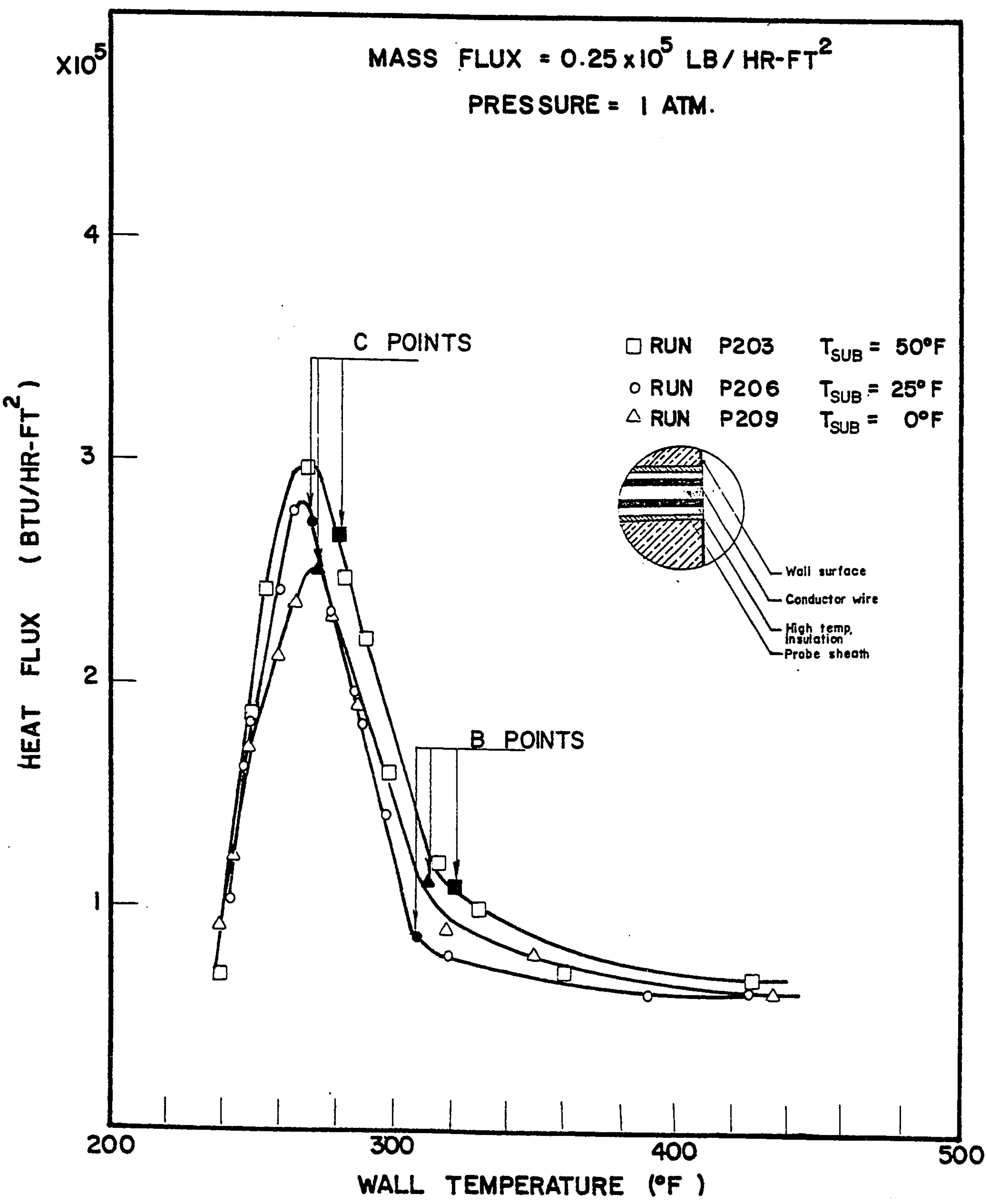

FIG.31 P200 RUN SERIES, 0.25×10^5 LB/HR.FT^2

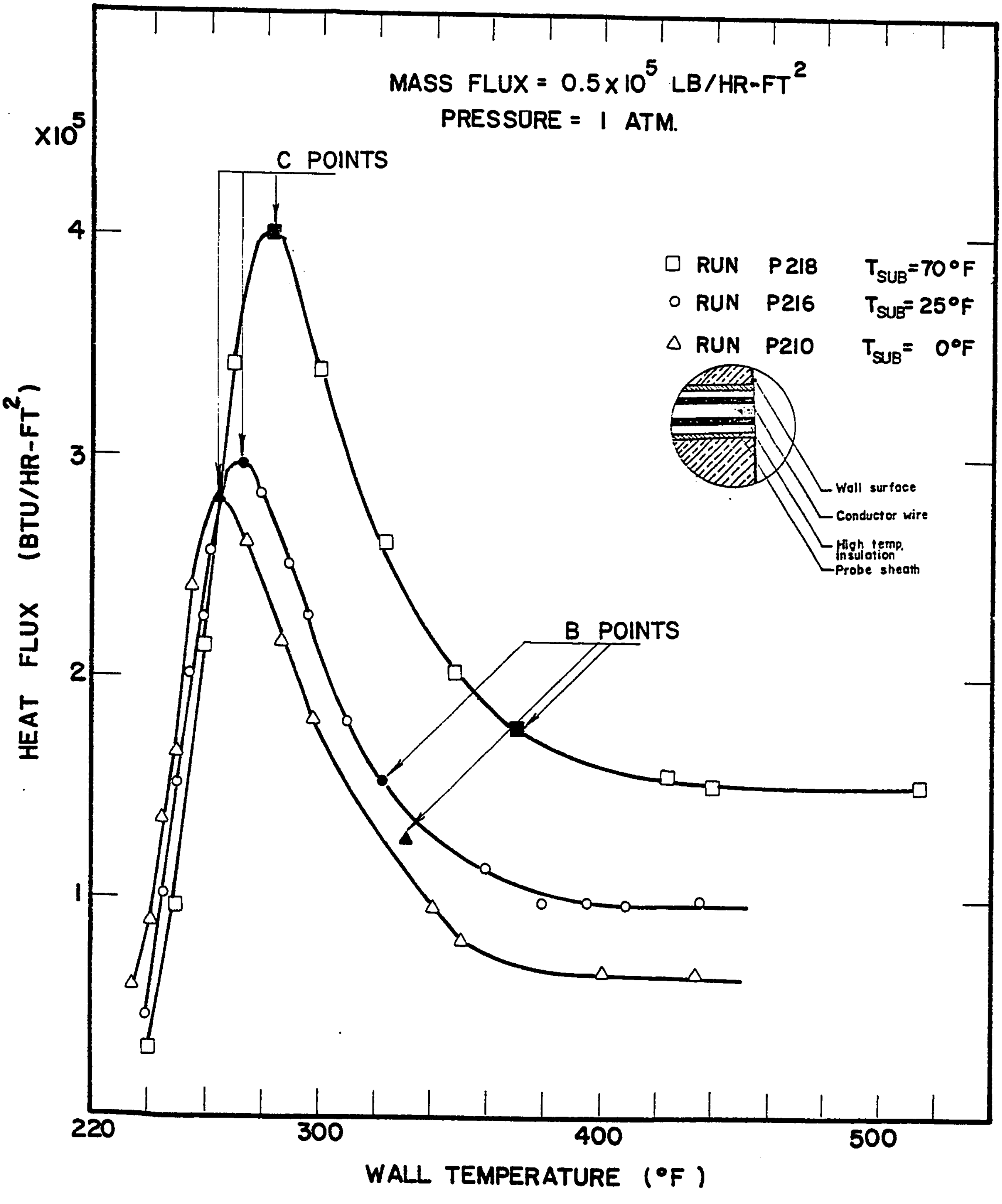

FIG. 32 P200 RUN SERIES, 0.50 X 10^5 LB/HR.FT^2

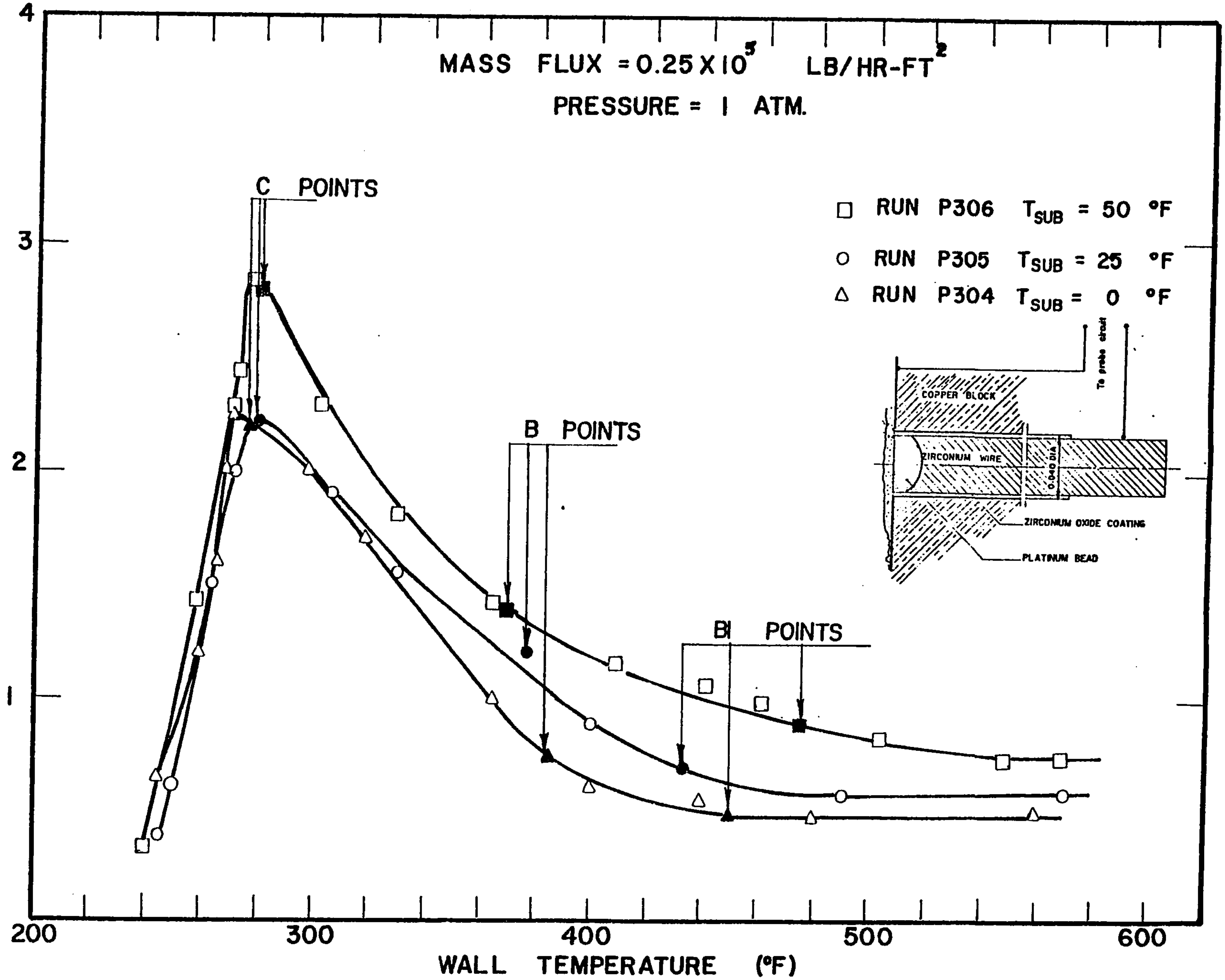

FIG. 33 P300 RUN SERIES, 0.25X10^5 LB/HR-FT^2

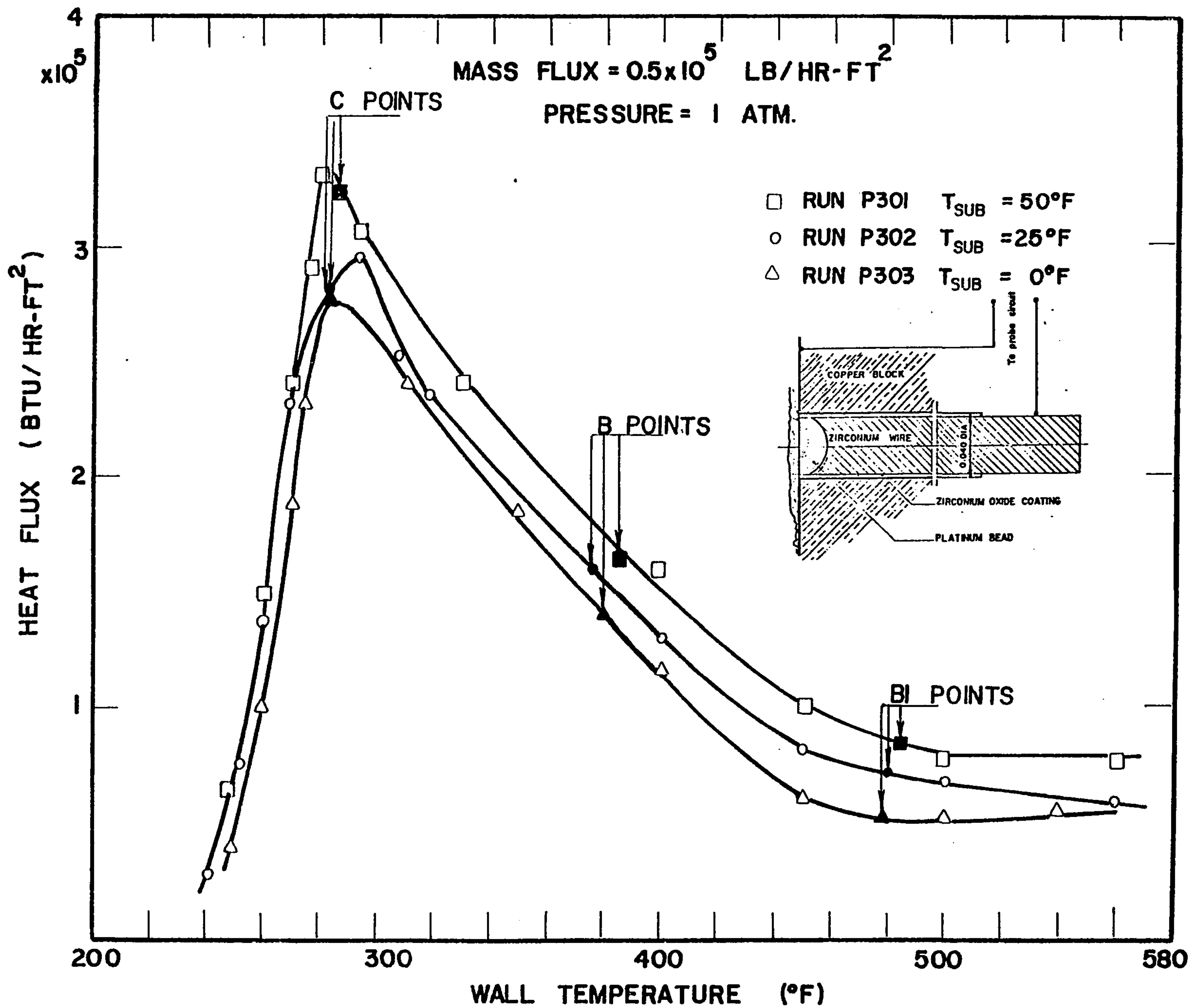

FIG.34 P300 RUN SERIES, 0.50X10^5 LB/HR.FT^2

Solid points (B and C) in Figs. 31-32, and (B,B1 and C) in Figs. 33-34, are obtained from the probe signals, and their meanings were explained in Chapter 4.

Before making any specific remarks, one would like to point out that the P300 series boiling curves are slightly shifted to the right of P200 series, though they were measured under the same conditions. This difference is believed to be due to surface effect. For example, oxidation and deposition of foreign matter on the heating surface enhance heat transfer. Berenson [23] observed this effect when he cleaned and lapped the surface (see run No. 10, Fig. 35).

On the basis of P200 and P300 series results, some remarks can be made in the following:

1. Both methods - temperature and electric measurements - gave identical locations of maximum heat flux (point C), at a surface temperature of approximately 280^{o}F in both series, within the range of the parameters used.

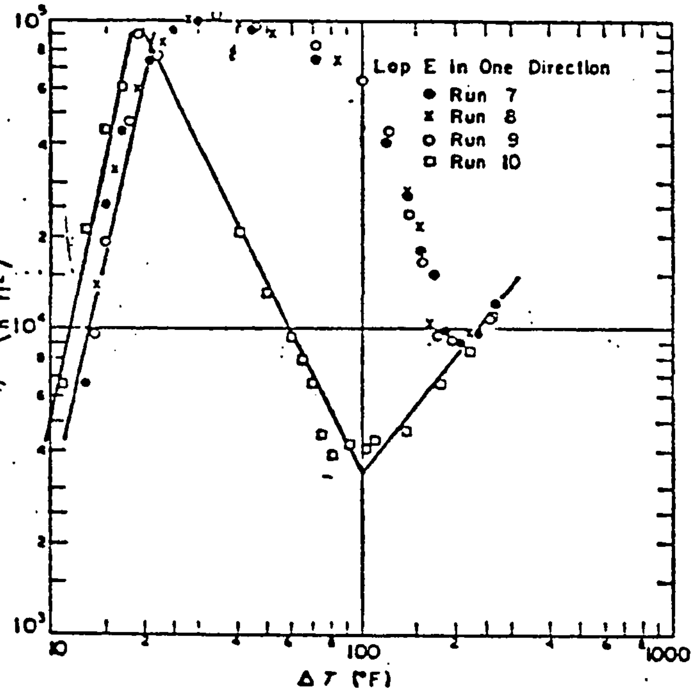

Copper-pentane test results: effect of surface cleanliness.

FIG.35 EFFECT OF SURFACE CONDITIONS ON BOILING CURVE

FROM BERENSON [23]

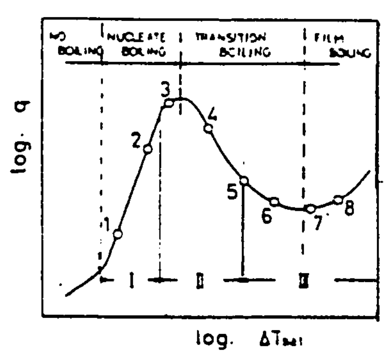

NO	ΔT_{sat} (°K)
1	14 8
2	17 2
3	35 5
4	PREDICTED
5	112
6	171
7	200
8	297

Generous classification of boiling mechanism based on the structure of vapor void.

FIG.36 CLASSIFICATION OF BOILING MECHANISM

FROM IIDA [15]

2. The two types of probe showed that a significant collapse of vapor film occurred in the transition boiling region of low degree of surface superheat (region BC).

3. The onset of local rewetting (point B1), was detected in the P300 series only. According to Figs. 33 and 34 , the liquid-solid contact appears at 440°F - 480°F, for mass fluxes 0.25 and 0.5×10^5 lbm/hr.ft^2. These points are suggested as the rewetting or Leidenfrost* points.

4. Since the liquid-wall contact area remained quite small up to point B, compared with a significant collapse of the vapor film (from B to C), it is possible that the film boiling exists in region BB1. This phenomenon has been observed by Iida [15]. He classified the three boiling regions (nucleate, transition, and film) on the boiling curve, according

*Leidenfrost temperature of a heated surface is the temperature above which the liquid is prevented from wetting the heated surface.

to the vapor void structure detected by means of an electric probe. This classification is shown in Fig. 36, where film boiling (region III) occupies a part of the transition region of high degree of surface superheat. Therefore, it appears that the transition from film boiling (dry surface with momentarily liquid-solid contact) to the transition boiling (partially wetted surface) does not occur at T_{min}.

5.6 - Conclusions

1. The applicability of electrical probes for detecting phase change on a heated surface has been studied under forced vertical flow conditions.

2. Probe-to-Wall measurements have been shown to be more informative than two-electrode measurements, especially in detecting liquid-solid contact in the film boiling regime.

3. The zirconium-platinum probe has proven to be advantageous over the thermocouple

probe due to its reliability and corrosion resistance, and it is recommended for future work.

4. Maximum heat flux points detected by the two types of probe are in good agreement with those available from boiling curves.

5. Onset of rewetting was detected by the Zirconium-Platinum probe at 440^{o} - $480^{o}F$, for mass fluxes 0.25 and $0.5x10^{5}$ $lbm/hr.ft^{2}$.

6. Intermittent liquid-solid contacts were detected in the film boiling regime.

5.7 - Suggestions for Future Work

1. Due to the limited range of flow parameters employed in the experiment, no correlation equation has been attempted to generalize the wall surface temperatures at the rewetting and maximum heat flux points. It is recommended for future studies that the zirconium-platinum probe be employed to determine such correlation, using a wider range of parameters.

2. An alternative arrangement for detecting the transition process, using the zirconium-platinum probe is suggested in Fig. 37. In this arrangement, the vapor film is not disturbed due to the smooth wall at the point of measurement.

3. It would also be very informative to detect the pressure change in the vapor film during the transition. This may be obtained, using the arrangement of Fig. 38. It is expected that the rupture of liquid-vapor interface, at the onset of rewetting, will produce a sudden change in the pressure of the vapor film.

4. In the present experimental set-up, inlet and outlet test section contact the fittings directly. These fittings need to be replaced by an insulated bracket so as to minimize axial conduction.

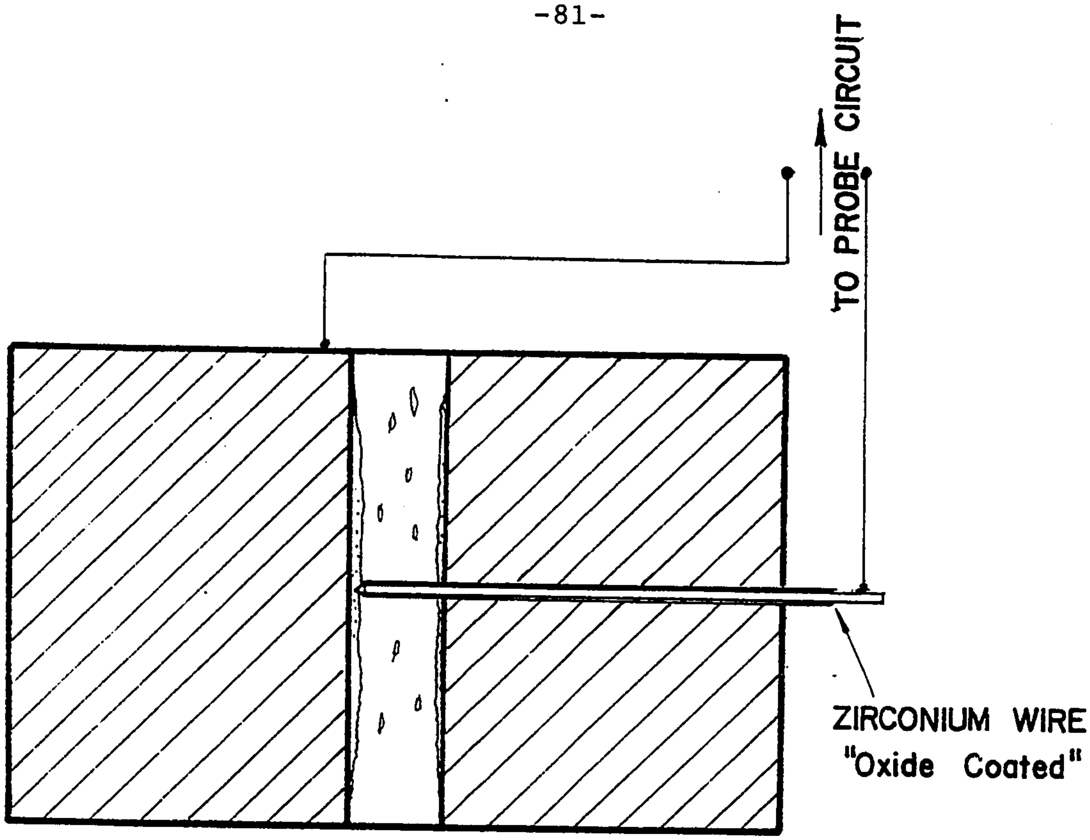

FIG. 37 ALTERNATIVE ARRANGEMENT FOR THE ZIRCONIUM PROBE

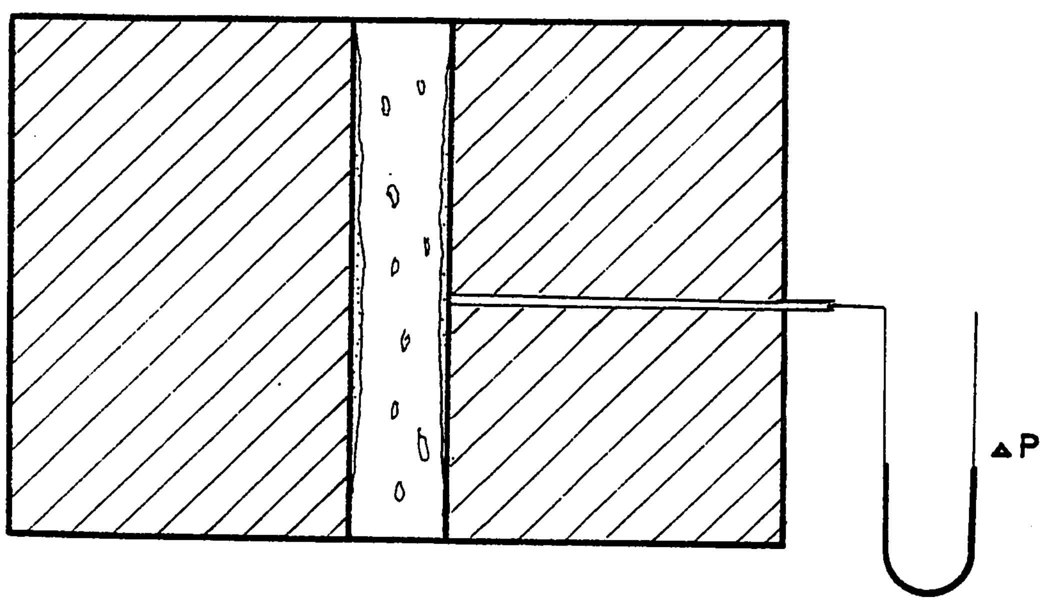

FIG. 38 DETECTING THE COLLAPSE BY PRESSURE MEASUREMENT

REFERENCES

1 . NUKIYAMA, S., "The Maximum and Minimum Values of the Heat Transmitted from Metal to Boiling Water Under Atmospheric Pressure", J. Soc. Mech. Engrs. Japan, 37, 367, 1934 .

2 . DREW, T.B., MUELLER, A.C., "Boiling", Trans. Am. Inst. Chem. Engrs., 33, 449, 1937 .

3 . GROENEVELD, D.C., and FUNG, K.K., "Forced Convective Transition Boiling Review of Literature and Comparison of Prediction Methods", A.E.C.L. - 5543, June, 1976.

4 . ILOEJE, O.C., PLUMMER, D.N. and ROHSENOW, W.M., "Transition from Film Boiling in Forced Convection Vertical Flow", MIT Technical Report 72718-78, 1972 .

5 . ILOEJE, O.C., PLUMMER, D.N., GRIFFITH, P., and ROHSENOW, W.M., "An Investigation of the Collapse and Surface Rewet in Film Boiling in Forced Vertical Flow", ASME paper 73-WA/HT-20, 1973 .

6 . COLLIER, J.G., "Post-Dryout Heat Transfer Under Low Flow and Low Quality Conditions", 1976 Water Reactor Safety Information Meeting, Gaithersburg, Washington, September 27-30, 1976.

7 . CHENG, S.C., and NG, W., "Transition Boiling Heat Transfer in Forced Vertical Flow Via a High Thermal Capacity Heating Process", the Letters in Heat and Mass Transfer Journal, Vol. 3, No. 4, pp 333-342, July/August, 1976.

8 . TACHIBANA, F. and SHINATARO, E., "Heat Transfer Problems in Quenching", Bulletin of JSME, 16, No. 91, 1973 .

9 . KALININ, E.K., YARKHO' S.A., BERLIN, I.I., KOCHELAEV, Yu.S., and KOSTYUK, V.V., "Investigation of the Crisis of Film Boiling in Channels", Paper Presented at the Winter Annual Meeting of ASME, 1969 .

10. SIMON, F.F., and SIMONEAU, R.J., "Transition from Film to Nucleate Boiling in Vertical Forced Flow", ASME paper 69-HT-26, 1969.

11. SPIEGLER, P., et al., "Onset of Stable Film Boiling and the Foam Limit", International Journal of Heat and Mass Transfer, Vol. 6, 1963.

12. HEWITT, G.F., KING, R.D., and LOVEGROVE, P.C., "Techniques for Liquid Film and Pressure Drop Studies in Annular Two-Phase Flow", AERE-R 3921, March, 1962.

13. GRIFFITH, P., "The Slug Annular Flow Regime Transition at Elevated Pressure", ANL - 6796, November, 1963.

14. HABERSTROH, R.E., and GRIFFITH, P., "The Slug-Annular Two-Phase Flow Regime Transition", ASME Paper 65-HT-52, 1965.

15. IIDA, Y., KOBAYASI, K., "An Experimental Investigation on the Mechanism of Pool Boiling Phenomena by a Probe Method", Proc. 4th Int. Heat Transfer Conference, Vol. 5, Paper B1.3, Versailles, 1970.

16. CHENG, S.C., RAGHEB, H., NG, W., and HENG, K.T., "Electric Probe to Detect Phase Change on the Wall", Special Report Under Contract with Argonne National Laboratory, Argonne, Illinois, Contract No. 31-109-38-3564, April, 1977.

17. BURGGRAF, O.R., "An Exact Solution of the Inverse Problem in Heat Conduction Theory and Applications", Journal of Heat Transfer, pp. 373-382, August, 1964.

18. CHENG, S.C., HENG, K.T., and NG, W., "A Technique to Construct a Boiling Curve from Quenching Data Considering Heat Loss", Int. J. of Multiphase Flow, Vol. 3, pp 495-499, September, 1977.

19. IBM System/360 Continuous System Modeling Program User's Manual Program No. 360 A-CX-16X, 1972.

20. CHENG, S.C., KULKARNI, K., and BIRTA L.G., "Insurge Transients from a Surge Tank Using CSMP", Simulation, Vol. 23, No. 4, pp 109-114, October, 1974 .

21. FIORI, M.P., and BERGLES, A.E., "Model of Critical Heat Flux in Subcooled Flow Boiling", MIT Mech. Eng. Dept. Rpt. DSR-70281-56, 1968 .

22. BRADFIELD, W.S., "Liquid-Solid Contact in Stable Film Boiling", I&EC Fundamentals, Vol. 5 No. 2, May, 1966.

23. BERENSON, P.J., "Experiments On Pool-Boiling Heat Transfer", Int. J. of Heat and Mass Transfer, Vol. 5, pp 985-999, 1962 .

24. CHENG, S.C., NG, W., HENG, K.T., RAGHEB, H., "Transition Boiling Heat Transfer in Forced Vertical Flow", Final Report, Under Contract with Argonne National Laboratory, Argonne, Illinois, Contract No. 31-109-38-3564, June, 1977.

25. HSU, Y.Y., and GRAHAM, R.W., "Transport Processes in Pool Boiling", McGraw-Hill Book Company, 1976 .

APPENDIX

A SAMPLE COMPUTER PROGRAM

```
****CONTINUOUS SYSTEM MODELING PROGRAM****

***PROBLEM INPUT STATEMENTS***

***********************************************************************
*                                       RUN  P215                     *
*                                                                     *
*                         MASS FLUX              =25000  LB/HR-SQ.FT. *
*                         DEGREE OF SUBCOOLING=   25 DEGREE F         *
*                                                                     *
***********************************************************************

/           DIMENSION R(30)
FIXED       N , NM1
PARAM       CP=0.092,RO=558.00,DO=4.0,DI=0.500,K=224.0
INITIAL
            NM1=8
            ALPHA=1.0/(0.23*3600.0)
            HCOE=6.0
            DIFT=DI/12.0
            RI=DI/(2.0*12.0)
            L=4.125/12.0
            H1=0.035/12.0
            H=1.715/(12.0*NM1)
            RA=RI+H1
            OUTA=3.14159* L*DO/12.0
            NADR=ALPHA/H
            S=ALPHA/H **2
            SS=ALPHA/(2.0*H)
            C1=(H+H1)/(2.0*ALPHA)
            C2=C1*RA*H*H1

***********************************************************************
*                                                                     *
*          UNITS OF THESE  PARAMETERS ARE AS FOLLOWED:-               *
*                                                                     *
*          CP   =BTU/LB-F          ,       ALPHA=SQ.FT./SEC.          *
*          K    =BTU/HR-FT-F       ,       RO   =LB/CU.FT             *
*          DI   =IN                ,       DO   =IN                   *
*          L    =FT                ,       H,H1 =FT                   *
*                                                                     *
***********************************************************************

            TCO=9.73
            TC5=9.73
            TC3=9.5
            TDIFF=19.0
            TCON=0.0
            TO   =NLFGEN(MVT,TCO)
            TEMP3=NLFGEN(MVT,TC3)
            TEMP5=NLFGEN(MVT,TC5)
            DUDT=(TEMP3-TO)/TDIFF
            DTDR=(TEMP5-TO)/(NM1*H)
```

```
        IC0=TO
        IC1=DTDR*H*1.0+TO
        IC2=DTDR*H*2.0+TO
        IC3=DTDR*H*3.0+TO
        IC4=DTDR*H*4.0+TO
        IC5=DTDR*H*5.0+TO
        IC6=DTDR*H*6.0+TO
        IC7=DTDR*H*7.0+TO
        IC8=DTDR*H*8.0+TO

************************************************************************
*                                                                      *
*              IC0, IC1, IC2, ..., IC8, ARE THE INITIAL                *
*              TEMPERATURES AT THE NODAL POINTS 0,1,...,8              *
*                                                                      *
************************************************************************

NOSORT
        DO 1 N=1,NM1
        R(N)=RA+N*H
        1 CONTINUE

************************************************************************
*                                                                      *
*              FUNCTION MVT IS A CONVERSION TABLE FOR                  *
*              MILLIVOLTS VS. TEMPERATURE.                             *
*                                                                      *
************************************************************************

 FUNCTION MVT=4.508,230.0,4.531,231.0,4.554,232.0,4.577,233.0,...
4.6,234.0,4.622,235.0,4.645,236.0,4.668,237.0,4.691,238.0,4.714,...
239.0,4.737,240.0,4.759,241.0,4.782,242.0,4.805,243.0,4.828,244.0,...
4.851,245.0,4.873,246.0,4.896,247.0,4.919,248.0,4.942,249.0,...
4.964,250.0,4.987,251.0,5.010,252.0,5.033,253.0,5.055,254.0,...
5.078,255.0,5.101,256.0,5.124,257.0,5.146,258.0,5.169,259.0,...
5.192,260.0,5.214,261.0,5.237,262.0,5.26,263.0,5.282,264.0,...
5.305,265.0,5.327,266.0,5.35,267.0,5.373,268.0,5.395,269.0,...
5.418,270.0,5.44,271.0,5.463,272.0,5.486,273.0,5.508,274.0,5.531,...
275.0,5.553,276.0,5.576,277.0,5.598,278.0,5.621,279.0,...
5.643,280.0,5.666,281.0,5.688,282.0,5.711,283.0,5.733,284.0,5.756,...
285.0,5.778,286.0,5.801,287.0,5.823,288.0,5.846,289.0,5.868,290.0,...
5.891,291.0,5.913,292.0,5.936,293.0,5.958,294.0,5.98,295.0,6.003,...
296.0,6.025,297.0,6.048,298.0,6.07,299.0,6.092,300.0,6.115,301.0,...
6.137,302.0,6.16,303.0,6.182,304.0,6.204,305.0,6.227,306.0,6.249,...
307.0,6.271,308.0,6.294,309.0,6.316,310.0,6.338,311.0,6.361,...
312.0,6.383,313.0,6.405,314.0,6.428,315.0,6.45,316.0,6.472,...
317.0,6.494,318.0,6.517,319.0,6.539,320.0,6.561,321.0,6.583,...
322.0,6.606,323.0,6.628,324.0,6.65,325.0,6.672,326.0,6.695,327.0,...
6.717,328.0,6.739,329.0,6.761,330.0,6.784,331.0,6.806,332.0,6.828,...
333.0,6.85,334.0,6.873,335.0,6.895,336.0,6.917,337.0,6.939,338.0,...
6.961,339.0,6.984,340.0,7.006,341.0,7.028,342.0,7.05,343.0,7.072,...
344.0,7.094,345.0,7.117,346.0,7.139,347.0,7.161,348.0,7.183,...
349.0,7.205,350.0,7.228,351.0,7.25,352.0,7.272,353.0,7.294,354.0,...
7.316,355.0,7.338,356.0,7.361,357.0,7.383,358.0,7.405,359.0,7.427,...
360.0,7.449,361.0,7.471,362.0,7.494,363.0,7.516,364.0,7.538,365.0,...
```

```
7.560,366.0,7.582,367.0,7.604,368.0,7.627,369.0,7.649,370.0,...
7.671,371.0,7.693,372.0,7.715,373.0,7.737,374.0,7.760,375.0,...
7.7820,376.0,7.804,377.0,7.826,378.0,7.848,379.0,7.870,380.0,...
7.893,381.0,7.915,382.0,7.937,383.0,7.959,384.0,7.981,385.0,...
8.003,386.0,8.026,387.0,8.046,388.0,8.070,389.0,8.092,390.0,...
8.114,391.0,8.137,392.0,8.159,393.0,8.181,394.0,8.203,395.0,...
8.225,396.0,8.248,397.0,8.270,398.0,8.292,399.0,8.314,400.0,...
8.336,401.0,8.359,402.0,8.381,403.0,8.403,404.0,8.425,405.0,...
8.448,406.0,8.470,407.0,8.492,408.0,8.514,409.0,8.537,410.0,...
8.559,411.0,8.581,412.0,8.603,413.0,8.626,414.0,8.648,415.0,...
8.670,416.0,8.692,417.0,8.715,418.0,8.737,419.0,8.759,420.0,...
8.782,421.0,8.804,422.0,8.826,423.0,8.849,424.0,8.871,425.0,...
8.893,426.0,8.916,427.0,8.938,428.0,8.960,429.0,8.983,430.0,...
9.005,431.0,9.027,432.0,9.050,433.0,9.072,434.0,9.094,435.0,...
9.117,436.0,9.139,437.0,9.161,438.0,9.184,439.0,9.206,440.0,...
9.229,441.0,9.251,442.0,9.273,443.0,9.296,444.0,9.318,445.0,...
9.341,446.0,9.363,447.0,9.385,448.0,9.408,449.0,9.430,450.0,...
9.453,451.0,9.475,452.0,9.498,453.0,9.520,454.0,9.543,455.0,...
9.565,456.0,9.588,457.0,9.610,458.0,9.633,459.0,9.655,460.0,...
9.678,461.0,9.700,462.0,9.723,463.0,9.745,464.0,9.768,465.0,...
9.790,466.0,9.813,467.0,9.835,468.0,9.858,469.0,9.880,470.0,...
9.903,471.0,9.926,472.0,9.948,473.0,9.971,474.0,9.993,475.0,...
10.016,476.0,10.038,477.0,10.061,478.0,10.084,479.0,10.106,480.0,...
10.129,481.0,10.151,482.0,10.174,483.0,10.197,484.0,10.219,485.0,...
10.242,486.0,10.265,487.0,10.287,488.0,10.310,489.0,10.333,490.0,...
10.355,491.0,10.378,492.0,10.401,493.0,10.423,494.0,10.446,495.0,...
10.469,496.0,10.491,497.0,10.514,498.0,10.537,499.0,10.560,500.0,...
10.582,501.0,10.605,502.0,10.628,503.0,10.650,504.0,10.673,505.0,...
10.696,506.0,10.719,507.0,10.741,508.0,10.764,509.0,10.787,510.0,...
10.810,511.0,10.833,512.0,10.855,513.0,10.878,514.0,10.901,515.0,...
10.924,516.0,10.947,517.0,10.969,518.0,10.992,519.0,11.015,520.0,...
11.038,521.0,11.061,522.0,11.083,523.0,11.106,524.0,11.129,525.0,...
11.152,526.0,11.175,527.0,11.198,528.0,11.221,529.0,11.243,530.0,...
11.266,531.0,11.289,532.0,11.312,533.0,11.335,534.0,11.358,535.0,...
11.381,536.0,11.404,537.0,11.426,538.0,11.449,539.0,11.472,540.0,...
11.495,541.0,11.518,542.0,11.541,543.0,11.564,544.0,11.587,545.0,...
11.610,546.0,11.633,547.0,11.656,548.0,11.679,549.0,11.702,550.0,...
11.725,551.0,11.748,552.0,11.770,553.0,11.793,554.0,11.816,555.0,...
11.839,556.0,11.862,557.0,11.885,558.0,11.908,559.0,11.931,560.0,...
11.954,561.0,11.977,562.0,12.000,563.0,12.023,564.0,12.046,565.0,...
12.069,566.0,12.092,567.0,12.115,568.0,12.138,569.0,12.161,570.0,...
12.184,571.0,12.207,572.0,12.230,573.0,12.254,574.0,12.277,575.0,...
12.300,576.0,12.323,577.0,12.346,578.0,12.369,579.0,12.392,580.0,...
12.415,581.0,12.438,582.0,12.461,583.0,12.484,584.0,12.507,585.0,...
12.530,586.0,12.553,587.0,12.576,588.0,12.599,589.0,12.623,590.0,...
12.646,591.0,12.669,592.0,12.692,593.0,12.715,594.0,12.738,595.0,...
12.761,596.0,12.784,597.0,12.807,598.0,12.831,599.0,12.854,600.0,...
12.877,601.0,12.900,602.0,12.923,603.0,12.946,604.0,12.969,605.0,...
12.992,606.0,13.016,607.0,13.039,608.0,13.062,609.0,13.085,610.0,...
13.224,616.0,13.247,617.0,13.270,618.0,13.293,619.0,13.317,620.0,...
```

```
13.340,621.0,13.363,622.0,13.386,623.0,13.409,624.0,13.433,625.0,...
13.456,626.0,13.479,627.0,13.502,628.0,13.525,629.0,13.549,630.0,...
13.572,631.0,13.595,632.0,13.618,633.0,13.641,634.0,13.665,635.0,...
13.688,636.0,13.711,637.0,13.734,638.0,13.757,639.0,13.781,640.0,...
13.804,641.0,13.827,642.0,13.850,643.0,13.874,644.0,13.897,645.0,...
13.920,646.0,13.943,647.0,13.967,648.0,13.990,649.0,14.013,650.0,...
14.036,651.0,14.060,652.0,14.083,653.0,14.106,654.0,14.129,655.0,...
14.153,656.0,14.176,657.0,14.199,658.0,14.222,659.0,14.246,660.0,...
14.269,661.0,14.292,662.0,14.316,663.0,14.339,664.0,14.362,665.0,...
14.385,666.0,14.409,667.0,14.432,668.0,14.455,669.0,14.479,670.0,...
14.502,671.0,14.525,672.0,14.548,673.0,14.572,674.0,14.595,675.0,...
14.618,676.0,14.642,677.0,14.665,678.0,14.688,679.0,14.712,680.0,...
14.735,681.0,14.758,682.0,14.782,683.0,14.805,684.0,14.828,685.0,...
14.852,686.0,14.875,687.0,14.898,688.0,14.922,689.0,14.945,690.0,...
14.968,691.0,14.992,692.0,15.015,693.0,15.038,694.0,15.062,695.0,...
15.085,696.0,15.108,697.0,15.132,698.0,15.155,699.0,15.178,700.0,...
15.202,701.0,15.225,702.0,15.248,703.0,15.272,704.0,15.295,705.0,...
15.318,706.0,15.342,707.0,15.365,708.0,15.389,709.0,15.412,710.0,...
15.435,711.0,15.459,712.0,15.482,713.0,15.505,714.0,15.529,715.0,...
15.552,716.0,15.576,717.0,15.599,718.0,15.622,719.0,15.646,720.0,...
15.669,721.0,15.693,722.0,15.716,723.0,15.739,724.0,15.763,725.0,...
15.786,726.0,15.810,727.0,15.833,728.0,15.856,729.0,15.880,730.0,...
15.903,731.0,15.927,732.0,15.950,733.0,15.974,734.0,15.997,735.0,...
16.020,736.0,16.044,737.0,16.067,738.0,16.091,739.0,16.114,740.0,...
16.138,741.0,16.161,742.0,16.184,743.0,16.208,744.0,16.231,745.0,...
16.255,746.0,16.278,747.0,16.302,748.0,16.325,749.0,16.349,750.0,...
16.372,751.0,16.395,752.0,16.419,753.0,16.443,754.0,16.466,755.0,...
16.489,756.0,16.513,757.0,16.536,758.0,16.560,759.0,16.583,760.0,...
16.607,761.0,16.630,762.0,16.654,763.0,16.677,764.0,16.700,765.0,...
16.724,766.0,16.747,767.0,16.771,768.0,16.794,769.0,16.818,770.0,...
16.841,771.0,16.865,772.0,16.888,773.0,16.912,774.0,16.935,775.0,...
16.959,776.0,16.982,777.0,17.006,778.0,17.029,779.0,17.053,780.0,...
17.076,781.0,17.100,782.0,17.123,783.0,17.147,784.0,17.170,785.0,...
17.194,786.0,17.217,787.0,17.241,788.0,17.264,789.0,17.288,790.0,...
17.311,791.0,17.335,792.0,17.358,793.0,17.382,794.0,17.406,795.0,...
17.429,796.0,17.453,797.0,17.476,798.0,17.500,799.0,17.523,800.0,...
17.547,801.0,17.570,802.0,17.594,803.0,17.617,804.0,17.641,805.0,...
17.664,806.0,17.688,807.0,17.711,808.0,17.735,809.0,17.759,810.0,...
17.782,811.0,17.806,812.0,17.829,813.0,17.853,814.0,17.876,815.0,...
17.900,816.0,17.923,817.0,17.947,818.0,17.971,819.0,17.994,820.0,...
18.018,821.0,18.041,822.0,18.065,823.0,18.088,824.0,18.112,825.0,...
18.136,826.0,18.159,827.0,18.183,828.0,18.206,829.0,18.230,830.0,...
18.253,831.0,18.277,832.0,18.301,833.0,18.324,834.0,18.348,835.0,...
18.371,836.0,18.395,837.0,18.418,838.0,18.442,839.0,18.466,840.0,...
18.489,841.0,18.513,842.0,18.536,843.0,18.560,844.0,18.584,845.0,...
18.607,846.0,18.631,847.0,18.654,848.0,18.678,849.0,18.702,850.0,...
18.725,851.0,18.749,852.0,18.772,853.0,18.796,854.0,18.820,855.0,...
18.843,856.0,18.867,857.0,18.890,858.0,18.914,859.0,18.938,860.0,...
18.961,861.0,18.985,862.0,19.008,863.0,19.032,864.0,19.056,865.0,...
```

```
19.079,866.0,19.103,867.0,19.127,868.0,19.150,869.0,19.174,870.0,...
19.197,871.0,19.221,872.0,19.245,873.0,19.268,874.0,19.292,875.0,...
19.316,876.0,19.339,877.0,19.363,878.0,19.386,879.0,19.410,880.0,...
19.434,881.0,19.457,882.0,19.481,883.0,19.505,884.0,19.528,885.0,...
19.552,886.0,19.576,887.0,19.599,888.0,19.623,889.0,19.646,890.0,...
19.670,891.0,19.694,892.0,19.717,893.0,19.741,894.0,19.765,895.0,...
19.788,896.0,19.812,897.0,19.836,898.0,19.859,899.0,19.883,900.0

*************************************************************************
*                                                                       *
*              INPUT VARIABLE TO THE MODEL                              *
*                                                                       *
*              FUNCTION (THIS) IS THE INPUT TEMPERATURE HISTORY         *
*              AS RECORDED BY THE THERMOCOUPLE.                         *
*                                                                       *
*                                                                       *
*************************************************************************
 FUNCTION THIS =0.0,9.73,19.0,9.50,35.0,9.3,50.0,9.1,79.0,8.5,...
100.0,8.19,120.0,7.69,138.0,7.30,156.0,6.9,169.0,6.6,179.0,6.31,...
186.0,6.1,189.0,6.0,190.0,5.96,191.0,5.90,192.0,5.83,193.0,5.7,...
193.7,5.6,194.0,5.55,195.0,5.4,196.0,5.3,197.0,5.22,198.0,5.19,...
199.0,5.15,200.0,5.12,201.0,5.1,203.0,5.08,207.0,5.0,213.0,4.9,...
221.0,4.8,230.0,4.7,242.0,4.6

DYNAMIC

*************************************************************************
*                                                                       *
*              CALCULATION OF THE TEMPERATURE DISTRIBUTION              *
*              ACROSS THE WALL.                                         *
*                                                                       *
*************************************************************************

        UU=NLFGEN(THIS,TIME)
        TT=NLFGEN(MVT,UU)
        TAMB=72.0-TCON
        T0=TT-TCON
        T1=INTGRL(IC1,TD1)
        T2=INTGRL(IC2,TD2)
        T3=INTGRL(IC3,TD3)
        T4=INTGRL(IC4,TD4)
        T5=INTGRL(IC5,TD5)
        T6=INTGRL(IC6,TD6)
        T7=INTGRL(IC7,TD7)
        T8=INTGRL(IC8,TD8)
        TD1=S*(T0-2.0*T1+T2)+SS*(T2-T0)/R(1)
        TD2=S*(T1-2.0*T2+T3)+SS*(T3-T1)/R(2)
        TD3=S*(T2-2.0*T3+T4)+SS*(T4-T2)/R(3)
        TD4=S*(T3-2.0*T4+T5)+SS*(T5-T3)/R(4)
        TD5=S*(T4-2.0*T5+T6)+SS*(T6-T4)/R(5)
        TD6=S*(T5-2.0*T6+T7)+SS*(T7-T5)/R(6)
        TD7=S*(T6-2.0*T7+T8)+SS*(T8-T6)/R(7)
        TD8=S*(2.0*T7-2.0*T8-2.0*HCOE*H*(T8-TAMB)/K )+SS*(-2.0*...
        HCOE*H*(T8-TAMB)/K )/R(8)
```

```
**********************************************************************
*                                                                    *
*             UTILISATION OF DERIVATIVE PACKAGE (DERIV)              *
*             TO COMPUTE HT FROM Q.                                  *
*                                                                    *
*             HT   = HEAT FLUX          BTU/HR-SQ.FT                 *
*             TW   = WALL TEMPERATURE DEGREE F                       *
*                                                                    *
**********************************************************************

         REVTEM=(TW*RI*H1+T0*RA*H1+T0*RA*H)/2.0
         SUM=(T1*R(1)+T2*R(2)+T3*R(3)+T4*R(4)+T5*R(5)+T6*R(6)...
         +T7*R(7)+T8*R(8)*0.5)*H+REVTEM
         DU0=DERIV(DUDT,T0)
         TW =(2.0*C2*DU0-2.0*RA*(T1-T0)*H1+2.0*RA*T0*H-T1*H1*H)/...
         (2.0*RA*H-H1*H)
         TIW=TCON+TW
         Q=2.0*3.14159*CP*RO* L*SUM
         QOUTW=OUTA*HCOE*(T8-TAMB)
         HTT=DERIV(0.0,Q)
         HTCU=HTT*3600.0
         HTN=-(HTCU+QOUTW)
         HT=HTN/(3.14159* L    *DIFT)
TERMINAL
         DO 120 N=1,NM1
         WRITE (6,111) R(N),H
         111  FORMAT ( 2(E14.6,5X))
         120  CONTINUE
         WRITE (6,112) TEMPS
         112  FORMAT (////, ' T-WALL=',F10.5)

**********************************************************************
*                                                                    *
*             SPECIFICATION OF DURATION OF SIMULATION RUN            *
*             AND OUTPUT PLOT OF HEAT FLUX VS. TIME                  *
*                                                                    *
**********************************************************************

TIMERT   FINTIM=242.0,DELT=0.1 ,PRDEL=1.0,OUTDEL=0.5
LABEL    HEAT TRANSFER  PER UNIT AREA PER UNIT TIME
METHOD   RKSFX
PRTPLT   HT(TW)
END
STOP
```

```
HEAT TRANSFER  PER UNIT AREA PER UNIT TIME

                                 MINIMUM              HT      VERSUS TIME              MAXIMUM
                               -1.8783E 04                                            3.1074E 05
   TIME             HT           I                                                        I          TW
1.5400E 02      1.0680E 05    --------------------+                                               3.3698E 02
1.5450E 02      1.0645E 05    --------------------+                                               3.3646E 02
1.5500E 02      1.0762E 05    --------------------+                                               3.3595E 02
1.5550E 02      1.0683E 05    --------------------+                                               3.3544E 02
1.5600E 02      1.0726E 05    --------------------+                                               3.3493E 02
1.5650E 02      1.0756E 05    --------------------+                                               3.3440E 02
1.5700E 02      1.0709E 05    --------------------+                                               3.3389E 02
1.5750E 02      1.0749E 05    --------------------+                                               3.3339E 02
1.5800E 02      1.0759E 05    --------------------+                                               3.3290E 02
1.5850E 02      1.0769E 05    --------------------+                                               3.3238E 02
1.5900E 02      1.0783E 05    --------------------+                                               3.3186E 02
1.5950E 02      1.0805E 05    --------------------+                                               3.3133E 02
1.6000E 02      1.0855E 05    --------------------+                                               3.3081E 02
1.6050E 02      1.0841E 05    --------------------+                                               3.3028E 02
1.6100E 02      1.0803E 05    --------------------+                                               3.2976E 02
1.6150E 02      1.0913E 05    --------------------+                                               3.2927E 02
1.6200E 02      1.0868E 05    --------------------+                                               3.2876E 02
1.6250E 02      1.0943E 05    --------------------+                                               3.2824E 02
1.6300E 02      1.0900E 05    --------------------+                                               3.2771E 02
1.6350E 02      1.0885E 05    --------------------+                                               3.2718E 02
1.6400E 02      1.0950E 05    --------------------+                                               3.2665E 02
1.6450E 02      1.0980E 05    --------------------+                                               3.2612E 02
1.6500E 02      1.0894E 05    --------------------+                                               3.2560E 02
1.6550E 02      1.0947E 05    --------------------+                                               3.2510E 02
1.6600E 02      1.0979E 05    --------------------+                                               3.2458E 02
1.6650E 02      1.0976E 05    --------------------+                                               3.2405E 02
1.6700E 02      1.1000E 05    --------------------+                                               3.2352E 02
1.6750E 02      1.1012E 05    --------------------+                                               3.2299E 02
1.6800E 02      1.1071E 05    --------------------+                                               3.2245E 02
1.6850E 02      1.1126E 05    --------------------+                                               3.2191E 02
1.6900E 02      1.1058E 05    --------------------+                                               3.2141E 02
1.6950E 02      1.1197E 05    --------------------+                                               3.2081E 02
1.7000E 02      1.1288E 05    --------------------+                                               3.2019E 02
1.7050E 02      1.1394E 05    ---------------------+                                              3.1957E 02
1.7100E 02      1.1496E 05    ---------------------+                                              3.1893E 02
1.7150E 02      1.1604E 05    ---------------------+                                              3.1829E 02
1.7200E 02      1.1657E 05    ---------------------+                                              3.1765E 02
1.7250E 02      1.1732E 05    ---------------------+                                              3.1704E 02
1.7300E 02      1.1859E 05    ---------------------+                                              3.1640E 02
1.7350E 02      1.1946E 05    ---------------------+                                              3.1573E 02
1.7400E 02      1.1964E 05    ----------------------+                                             3.1507E 02
1.7450E 02      1.2173E 05    ----------------------+                                             3.1439E 02
1.7500E 02      1.2233E 05    ----------------------+                                             3.1371E 02
1.7550E 02      1.2290E 05    ----------------------+                                             3.1306E 02
```

HEAT TRANSFER PER UNIT AREA PER UNIT TIME

MINIMUM -1.8783E 04   HT VERSUS TIME   MAXIMUM 3.1074E 05

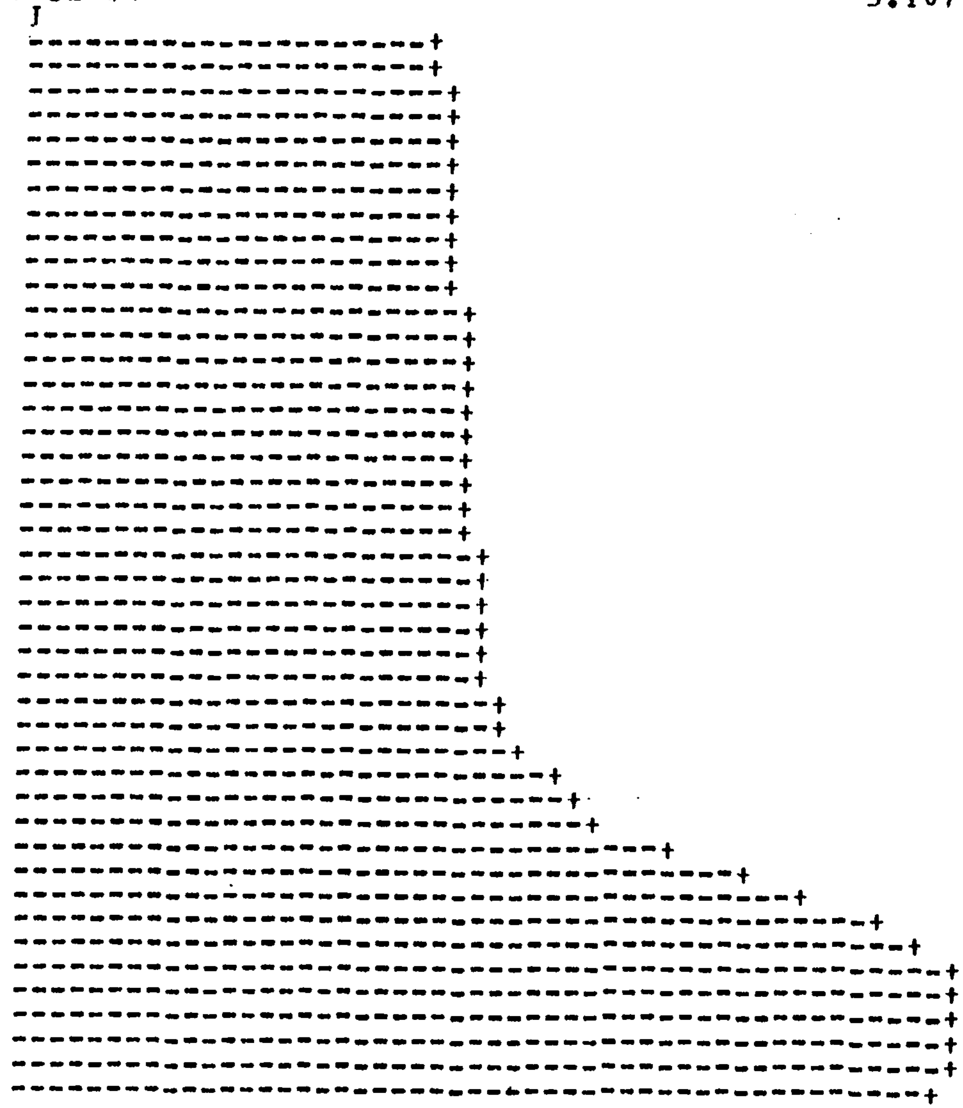

TIME	HT	TW
1.7600E 02	1.2417E 05	3.1238E 02
1.7650E 02	1.2465E 05	3.1168E 02
1.7700E 02	1.2647E 05	3.1097E 02
1.7750E 02	1.2679E 05	3.1029E 02
1.7800E 02	1.2815E 05	3.0960E 02
1.7850E 02	1.2882E 05	3.0888E 02
1.7900E 02	1.3019E 05	3.0815E 02
1.7950E 02	1.3034E 05	3.0747E 02
1.8000E 02	1.3056E 05	3.0683E 02
1.8050E 02	1.3154E 05	3.0616E 02
1.8100E 02	1.3249E 05	3.0547E 02
1.8150E 02	1.3289E 05	3.0478E 02
1.8200E 02	1.3333E 05	3.0412E 02
1.8250E 02	1.3361E 05	3.0346E 02
1.8300E 02	1.3440E 05	3.0277E 02
1.8350E 02	1.3568E 05	3.0207E 02
1.8400E 02	1.3532E 05	3.0138E 02
1.8450E 02	1.3585E 05	3.0073E 02
1.8500E 02	1.3670E 05	3.0004E 02
1.8550E 02	1.3745E 05	2.9935E 02
1.8600E 02	1.3723E 05	2.9869E 02
1.8650E 02	1.3943E 05	2.9794E 02
1.8700E 02	1.4098E 05	2.9718E 02
1.8750E 02	1.4132E 05	2.9641E 02
1.8800E 02	1.4215E 05	2.9568E 02
1.8850E 02	1.4343E 05	2.9490E 02
1.8900E 02	1.4401E 05	2.9413E 02
1.8950E 02	1.4663E 05	2.9324E 02
1.9000E 02	1.4993E 05	2.9227E 02
1.9050E 02	1.5836E 05	2.9094E 02
1.9100E 02	1.6806E 05	2.8938E 02
1.9150E 02	1.7451E 05	2.8781E 02
1.9200E 02	1.8224E 05	2.8610E 02
1.9250E 02	2.0919E 05	2.8322E 02
1.9300E 02	2.3512E 05	2.7969E 02
1.9350E 02	2.5377E 05	2.7631E 02
1.9400E 02	2.7870E 05	2.7250E 02
1.9450E 02	2.9436E 05	2.6883E 02
1.9500E 02	3.0701E 05	2.6551E 02
1.9550E 02	3.0801E 05	2.6300E 02
1.9600E 02	3.0681E 05	2.6107E 02
1.9650E 02	3.1058E 05	2.5913E 02
1.9700E 02	3.0952E 05	2.5752E 02
1.9750E 02	2.9796E 05	2.5669E 02

HEAT TRANSFER PER UNIT AREA PER UNIT TIME

MINIMUM -1.8783E 04 — HT VERSUS TIME — MAXIMUM 3.1074E 05

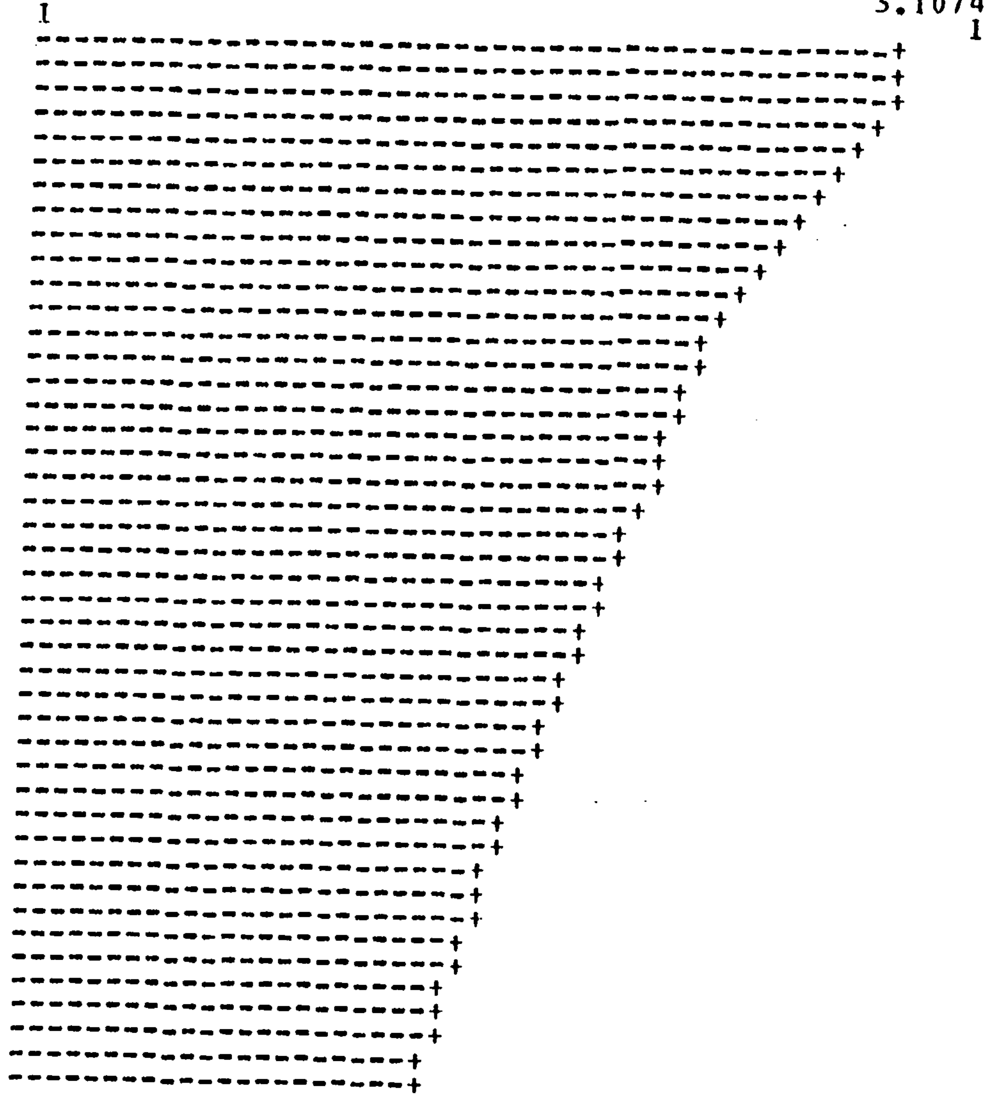

TIME	HT	TW
1.9800E 02	2.8325E 05	2.5648E 02
1.9850E 02	2.8435E 05	2.5565E 02
1.9900E 02	2.8316E 05	2.5475E 02
1.9950E 02	2.7703E 05	2.5408E 02
2.0000E 02	2.7033E 05	2.5355E 02
2.0050E 02	2.6338E 05	2.5314E 02
2.0100E 02	2.5578E 05	2.5285E 02
2.0150E 02	2.4886E 05	2.5261E 02
2.0200E 02	2.4153E 05	2.5245E 02
2.0250E 02	2.3321E 05	2.5237E 02
2.0300E 02	2.2532E 05	2.5236E 02
2.0350E 02	2.2181E 05	2.5209E 02
2.0400E 02	2.1753E 05	2.5180E 02
2.0450E 02	2.1359E 05	2.5147E 02
2.0500E 02	2.1048E 05	2.5107E 02
2.0550E 02	2.0748E 05	2.5063E 02
2.0600E 02	2.0442E 05	2.5017E 02
2.0650E 02	2.0201E 05	2.4968E 02
2.0700E 02	1.9986E 05	2.4914E 02
2.0750E 02	1.9469E 05	2.4880E 02
2.0800E 02	1.9042E 05	2.4846E 02
2.0850E 02	1.8650E 05	2.4812E 02
2.0900E 02	1.8357E 05	2.4778E 02
2.0950E 02	1.8008E 05	2.4742E 02
2.1000E 02	1.7666E 05	2.4708E 02
2.1050E 02	1.7326E 05	2.4676E 02
2.1100E 02	1.6971E 05	2.4645E 02
2.1150E 02	1.6629E 05	2.4614E 02
2.1200E 02	1.6301E 05	2.4585E 02
2.1250E 02	1.6005E 05	2.4555E 02
2.1300E 02	1.5656E 05	2.4527E 02
2.1350E 02	1.5427E 05	2.4499E 02
2.1400E 02	1.5118E 05	2.4471E 02
2.1450E 02	1.4803E 05	2.4444E 02
2.1500E 02	1.4537E 05	2.4416E 02
2.1550E 02	1.4218E 05	2.4389E 02
2.1600E 02	1.4031E 05	2.4362E 02
2.1650E 02	1.3710E 05	2.4336E 02
2.1700E 02	1.3401E 05	2.4312E 02
2.1750E 02	1.3138E 05	2.4288E 02
2.1800E 02	1.2923E 05	2.4265E 02
2.1850E 02	1.2646E 05	2.4243E 02
2.1900E 02	1.2380E 05	2.4221E 02
2.1950E 02	1.2117E 05	2.4200E 02

HEAT TRANSFER PER UNIT AREA PER UNIT TIME

MINIMUM -1.8783E 04 HT VERSUS TIME MAXIMUM 3.1074E 05

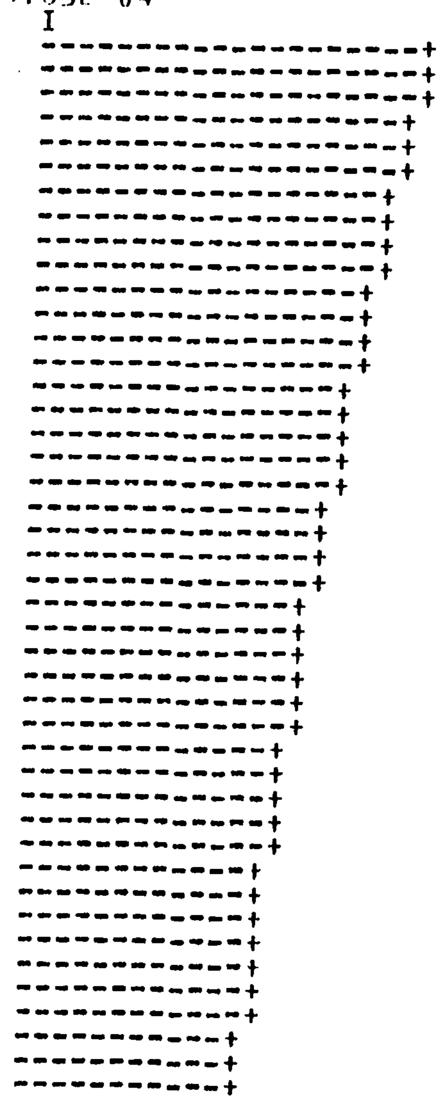

TIME	HT	TW
2.2000E 02	1.1860E 05	2.4180E 02
2.2050E 02	1.1570E 05	2.4160E 02
2.2100E 02	1.1404E 05	2.4140E 02
2.2150E 02	1.1216E 05	2.4117E 02
2.2200E 02	1.1002E 05	2.4093E 02
2.2250E 02	1.0787E 05	2.4071E 02
2.2300E 02	1.0612E 05	2.4048E 02
2.2350E 02	1.0411E 05	2.4026E 02
2.2400E 02	1.0269E 05	2.4003E 02
2.2450E 02	1.0086E 05	2.3980E 02
2.2500E 02	9.9536E 04	2.3956E 02
2.2550E 02	9.8035E 04	2.3932E 02
2.2600E 02	9.6085E 04	2.3909E 02
2.2650E 02	9.4623E 04	2.3886E 02
2.2700E 02	9.2750E 04	2.3865E 02
2.2750E 02	9.1619E 04	2.3843E 02
2.2800E 02	8.9707E 04	2.3821E 02
2.2850E 02	8.8849E 04	2.3800E 02
2.2900E 02	8.7170E 04	2.3779E 02
2.2950E 02	8.5862E 04	2.3757E 02
2.3000E 02	8.4613E 04	2.3736E 02
2.3050E 02	8.3167E 04	2.3717E 02
2.3100E 02	8.1663E 04	2.3697E 02
2.3150E 02	8.0022E 04	2.3678E 02
2.3200E 02	7.8752E 04	2.3659E 02
2.3250E 02	7.7501E 04	2.3641E 02
2.3300E 02	7.6308E 04	2.3622E 02
2.3350E 02	7.4822E 04	2.3604E 02
2.3400E 02	7.3941E 04	2.3586E 02
2.3450E 02	7.2181E 04	2.3569E 02
2.3500E 02	7.1651E 04	2.3551E 02
2.3550E 02	7.0457E 04	2.3534E 02
2.3600E 02	6.8345E 04	2.3517E 02
2.3650E 02	6.8068E 04	2.3501E 02
2.3700E 02	6.6502E 04	2.3485E 02
2.3750E 02	6.5541E 04	2.3469E 02
2.3800E 02	6.4190E 04	2.3453E 02
2.3850E 02	6.3385E 04	2.3437E 02
2.3900E 02	6.2482E 04	2.3422E 02
2.3950E 02	6.1149E 04	2.3406E 02
2.4000E 02	6.0597E 04	2.3390E 02
2.4050E 02	5.9635E 04	2.3375E 02
2.4100E 02	5.8263E 04	2.3360E 02
2.4150E 02	5.7066E 04	2.3346E 02